KAUNAS UNIVERSITY OF TECHNOLOGY

FACULTY OF MATHEMATICS AND NATURAL SCIENCES

Miglė Staliulionytė

INVESTIGATION OF PROPERTIES OF RADIOSENSITIVE HYDROGELS

Master's Final Degree Project

Supervisor
Doc. dr. Judita Puišo

KAUNAS, 2018

KAUNAS UNIVERSITY OF TECHNOLOGY

FACULTY OF MATHEMATICS AND NATURAL SCIENCES

INVESTIGATION OF PROPERTIES OF RADIOSENSITIVE HYDROGELS

Master's Final Degree Project

Medical Physics (code 621B92002)

Supervisor

Doc. dr. Judita Puišo

Consultant

Prof. dr. Diana Adlienė

Reviewer

Lekt. dr. Darius Virbukas

Project made by

Miglė Staliulionytė

KAUNAS, 2018

KAUNAS UNIVERSITY OF TECHNOLOGY

FACULTY OF MATHEMATICS AND NATURAL SCIENCES

(Faculty)

MIGLĖ STALIOLIONYTĖ

(Student's name, surname)

Medical Physics (code 621B92002)

(Title and code of study programme)

'Development of slab phantom prototype for the investigation of the doses to lower mandibular during low energy X-ray therapy'

DECLARATION OF ACADEMIC INTEGRITY

___ _____ 20 ___

Kaunas

I confirm that the final project of mine, Miglė Staliulionytė, on the topic 'Investigation of Properties of Radiosensitive Hydrogels' is written completely by myself; all the provided data and research results are correct and have been obtained honestly. None of the parts of this thesis have been plagiarised from any printed, Internet-based or otherwise recorded sources. All direct and indirect quotations from external resources are indicated in the list of references. No monetary funds (unless required by law) have been paid to anyone for any contribution to this project.

I fully and completely understand that any discovery of any manifestations/case/facts of dishonesty inevitably results in me incurring a penalty according to the procedure(s) effective at Kaunas University of Technology.

_____ _____

(name and surname filled in by hand) *(signature)*

TABLE OF CONTENTS

Table of contents 4
Summary 5
Santrauka 6
List of abbreviations 7
List of tables 9
List of figures 10
Introduction 12
1. Theoretical Review 14
1.1 Ionizing Radiation in the medicine 14
1.2 Interaction of radiation with matter 15
1.3 Radiation dosimetry systems 18
1.4 Fricke dosimetry 22
1.4.1 Fricke gel preparation and composition 23
1.5 Polymer gel dosimetry 25
1.5.1 Chemical principles of polymer gel dosimetry 25
1.5.2 Polymer gels fabrication and composition 29
1.5.3 Dose evaluation in polymer gel dosimeters 35
1.5.4 Applications of polymer gel dosimetry 37
1.6 Gel dosimeters and nanotechnology 40
1.6.1 Nanoparticles synthesis 42
2. Materials and methods 44
2.1 Gel preparation 44
2.2 Silver NPs synthesis and incorporation in gel 45
2.3 Gel irradiation 47
2.4 Evaluation of x-ray impact on gel 47
3. Results and discusions 52
Conclusions 72
References 73
Appendix 1 77

Miglė Staliulionytė. Investigation of Properties of Radiosensitive Hydrogels. Master's (Final Degree Project / supervisor doc. dr. Judita Puišo; Faculty of Matematics and Natural Sciences, Kaunas University of Technology.

Study field and area (study field group): Biomedical Sciences, Medicine and Health.

Keywords:*3D dosimetry, polymer gels dosimetry, MAGIC, nanoparticles.*

Kaunas, 2018. 77 pages.

SUMMARY

Polymer gel dosimetry is widely used for 3D dose distribution investigations, because dose gels are near tissue equivalent, dose sensitive and represent dosimeter and phantom at once. Polymer gels are perfect tool for investigation of the absorbed dose enhancement effects in tumor volume. These effects are explored in radiotherapy and can be achieved incorporating nanoparticles into the tumor. Incorporated nanoparticles enhance radiation absorption capability of irradiated gels. Since the gels are tissue equivalent polymer gels may be used for in vitro dose investigations.

The aim of this research was to investigate photon irradiated MAGIC (methacrylic acid in gelatin initiated by copper) gels of different concentrations containing silver nanoparticles. Properties of dose gels were investigated using film dosimetry system, UV-VIS spectroscopy and semiconductor detectors.

It was shown, that incorporation of silver nanoparticles in MAGIC gels led to better radiation absorption as compared to MAGIC gels without nanoparticles. Additionally the search for optimal methacrylic acid concentration was performed in order to sustain stable and homogeneous gel consistency. It was found that the gel, containing methacrylic acid concentration of 7% was mostly sensitive for irradiation. The impact of silver nanoparticles on radiation absorption properties of irradiated gels was also examined in this research.

Experimental results revealed that the best absorption of ionizing radiation was recorded in MAGIC (NPs 2mM) gel and X-ray absorption coefficient of this gel was 26.6 % at 5Gy. The highest X-ray absorption at 2 Gy was observed in MAGIC (NPs 20mM) gel.

It was also found that additional nanoparticles have been produced through radiolysis in irradiated gels. These nanoparticles contributed to the absorbed dose enhancement by ~1.6%.

Miglė Staliulionytė. Jonizuojančiajai Spinduliuotei jautrių hidrogelių savybių tyrimas. Magistro baigiamasis projektas / vadovas doc. dr. Judita Puišo; Kauno technologijos universitetas, matematikos ir gamtos mokslų fakultetas.

Studijų kryptis ir sritis (studijų krypčių grupė): Biomedicinos mokslai (02B), medicina ir sveikata.

Reikšminiai žodžiai: *3D dozimetrija, polimeriniai geliniai dezimetrai, MAGIC, nanodalelės*

Kaunas, 2018. 77 puslapiai.

SANTRAUKA

Polimerinių gelių dozimetrija yra plačiai naudojama 3D dozių paskirstymo tyrimams, nes šie geliai yra beveik lygiaverčiai audiniui, jautrūs dozei ir tuo pat metu atlieka dozimetro ir fantomo funkcijas. Polimeriniai geliai yra puikus įrankis tiriant dozių sugeries didinimo poveikį auglio tūryje. Didesnė sugertoji dozė navike spindulinės terapijos metu gali būti pasiekiama įterpiant nano dalels į naviką. Įterptos nanodalelės sustiprina spinduliuotės sugertį apšvitintuose geliuose. Kadangi geliai yra lygiaverčiai biologiniam audiniui, jie gali būti in vitro dozių tyrimuose.

Šio darbo tikslas buvo ištirti fotonais apšvitintus įvairių koncentracijų MAGIC (metakrilo rūgštis+želatina+varis) gelius, kurių sudėtyje yra sidabro nanodalelių. Gelių savybės buvo tiriamos naudojant fimus, UV-VIS spektroskopiją ir puslaidininkinius detektorius.

Buvo parodyta, kad sidabro nanodalelių įterpimas MAGIC gelyje pagerina spinduliuotės absorbciją, lyginant su MAGIC geliais be nanodalelių. Be to, siekiant palaikyti stabilią ir homogenišką gelio konsistenciją, buvo parinkta optimali metakrilo rūgšties koncentracija. Nustatyta, kad gelis, kuriame metakrilo rūgšties koncentracija yra 7%, yra jautriausias fotoninei apšvitai. Šiame tyrime taip pat buvo nagrinėjamas sidabro nanodalelių poveikis apšvitintų gelių rentgenoabsorbcinėms savybėms.

Eksperimento rezultatai parodė, kad geriausia jonizuojančiosios spinduliuotės sugertimi pasižymėjo MAGIC (NP 2 mM) gelis. Jo rentgeno absorbcijos koeficientas buvo 26,6% esant 5 Gy apšvitai. Didžiausias rentgeno absorbcijos koeficientas esant 2 Gy apšvitai buvo stebima MAGIC (NP 20 mM) gelyje.

Taip pat nustatyta, kad radiolizės metu apšvitintose gelyje buvo sintezuojamos papildomos nanodalelės. Šių nanodalelių indėlis į sugertos dozės didinimą ~ 1,6%.

LIST OF ABBREVIATIONS

3D –Three Dimensions.

3DCRT – Three Dimensional Conformal Radiation Therapy

AscA – Ascorbic Acid.

BANANA – N,N-methylene-bis-acrylamide, acrylamide, nitrous oxide, and agarose gel.

BANG – Bisacrylamide, Nitrogen and Aqueous Gelatin gel.

BIS - N,N'-methylene-bis-acrylamide.

BNCT – Boron Neutron Capture Therapy.

CTDI – Computed Tomography Dose Index.

CT – Computed Tomography.

HDR – High Dose Rate.

DEF – Dose Enhancement Factor.

DNA – Deoxyribonucleic Acid.

HEA – 2 –hydroxyethylacrylate.

HEMA - 2-Hydroxyethyl Methacrylate.

IGRT – Image Guided Radiation Therapy.

IMRT – Intensity Modulated Radiation Therapy.

IR – Ionizing Radiation.

LET – linear energy transfe

MAA – Methacrylic Acid.

MAG – Methacrylic Acid Based Gel.

MAGAT– Methacrylic Acid, Gelatine and Tetrakis gel.

MAGIC - Methacrylic and Ascorbic Acid in Gelatin Initiated by Copper.

MAGICA – Methacrylic and Ascorbic Acid in Gelatin Initiated by Copper with Agarose.

MRI – Magnetic Resonance Tomography.

NIPAM – N-isopropylacrylamide

nMAG – Normoxic Methacrylic Acid and Gelatine gel.

NMR – Nuclear Magnetic Resonance.

nPAG – Normoxic , Gelatin and Tetrakis gel.

NPs – Nanoparticles.

OSL – Optically Stimulated Luminescence.

PAG – Polyacrylamide Based Gel.

PAGAT – Polyacrylamide, Gelatin and Tetrakis Gel.

PET – Positron Emission Tomography.

PVA - Polyvinyl Alcohol.

ROS – Reactive Oxygen Spieces.

SBRT – Stereotactic Body Radiation Therapy.

SPECT – Single Photon Emission Computed Tomography.

SWDP – Slice Width Dose Profile.

TGMEMA – monomethacrylate.

THPC - Tetrakis (hydroxymethyl) phosphonium chloride

TLD – Thermoluminescent Dosimetry/Dosimeter.

UV-VIS – Ultraviolet-Visible Spectroscopy.

VIPAR – N-vinylpyrrolidone, Argon gel.

LIST OF TABLES

Table 1. Applications of IR in medicine..... 6

Table 2. Main parameters of IR used in medical procedures. 6

Table 3. Qantities used in radiation measurements. 20

Table 4. Advantages and disadvantages of main radiation dosimeters 24

Table 5. Some typical recipes with concentrations of main constituents for the most common Fricke and Fricke gel dosimeters with representative chemical yields. 30

Table 6. Summary of polymer gel dosimeters..... 34

Table. 7. Mass density, electron density, for MAG, PAG, MAGIC gel, water, human muscle tissue, bone, lung and fat. 37

Table 8. Chemical composition of 25g of each investigated gel..... 47

Table 9. Summary of trendline equations coefficients of gels. 70

LIST OF FIGURES

Fig. 1. Iliustration of different radiation interaction with matter mechanisms 18
Fig.2. Structure of the different film 21
Fig.3. Schematic representation of photon interaction with dosimetric gels. 27
Fig.4. R2 for MAGAS gels containing different concentrations of ascorbic acid (a) and N-acetyl-cysteine (b) 29
Fig.5. The dependence of R2 and of optical attenuation on dose for gels with different THPC concentration 30
Fig.6. Chemical structures of different monomers used in polymer gel 33
Fig.7. Radiotheraphy techniques where polymer gel dosimetry is applied 38
Fig.8. Human head gel phantom (BANG) irradiated with Gammaknife treatment unit dose distribution 39
Fig.9. Schematic illustration of radiation interaction processes with nanoparticles 41
Fig.10. Gel preparation in fume hood 46
Fig. 11. Gels irradiation with UV source 47
Fig.12. Accumulated nanoparticles concentration in different organs after injection 48
Fig.13. GafChromic RTQA2 film irradiated with different ionizing radiation doses 49
Fig.14. GafChromic EBT2 film irradiated with different ionizing radiation doses 49
Fig.15. Scheme of gels measurements using film. 49
Fig.16. Semiconductor dosimeter 50
Fig.17. Transmission measurement using semiconductor detector 50
Fig.18. UV-VIS spectrometer USB4000. 51
Fig.19. Scheme of spectrometric measurements 50
Fig.20. MAGIC(S) gel before and after irradiation 53
Fig.21. MAGIC(S) gel examination results using film 54
Fig.22. MAGIC(S) gel examination results using film 54
Fig.23. MAGIC(S) dosimetric gel response to irradiation dose at 550nm 55
Fig.24. Gelatin($AgNO_3$) gels after irradiation 55
Fig.25. Gelatin(NPs1mM) gels after irradiation 55
Fig.26. Gelatin($AgNO_3$) and Gelatin(NPs1mM) examination using film 56
Fig.27. Gelatin($AgNO_3$) and Gelatin(NPs1mM) gels examination using film 56
Fig.28. Comparison between Gelatin(AgNO3) and Gelatin(NPs1mM) gels UV-VIS spectrum 57
Fig.29. MAGIC(3%) gel after irradiation. 57
Fig.30. MAGIC(6%) gel after irradiation 58

Fig.31. MAGIC(9%) gel after irradiation. 58
Fig.32. MAGIC(3%) gel measurements using film 58
Fig.33. MAGIC(6%) gel measurements using film 59
Fig.34. MAGIC(9%) gel measurements using film 59
Fig.35. Dose sensitivity curves for MAGIC(3%), MAGIC(6%) and MAGIC(9%) gels evaluated using GafChromic films 60
Fig.36. X-ray absorption coefficient values of MAGIC(6%) gel 61
Fig.37. Spectrometric measurements of MAGIC(3%), MAGIC(9%) and MAGIC(6%) gels 62
Fig.38. Comparison of X-ray absorption coefficient values in gels with different methacrylic acid concentrations. Measurements were performed at 2 Gy level. 62
Fig.39. MAGIC(NPs10mM) gel after irradiation 63
Fig.40. MAGIC(NPs20mM) gel after irradiation 63
Fig.41. Comparison between MAGIC(NPs10mM) and MAGIC(NPs20mM) gel measurements using film 64
Fig.42. X-ray transmission in MAGIC(NPs10mM) and MAGIC(NPS20mM) gels irradiated with 2 Gy dose, measured using semiconductor detector. 64
Fig.43. UV-VIS spectrum of MAGIC(NPs2mM) gel 65
Fig.44. MAGIC(NPs2mM) gel after irradiation 66
Fig.45. Results of MAGIC(NPs2mM) gel with film 66
Fig.46. X-ray absorption coefficient values in MAGIC(NPs2mM) gel 67
Fig.47. MAGIC(NPs1mM) gel before and after irradiation 67
Fig.48. MAGIC(NPs5mM) gel before and after irradiation 68
Fig.49. MAGIC(NPs1mM) dose measurements results with film 68
Fig.50. MAGIC(NPs5mM) dose measurements results with film 69
Fig.51. Comparison between MAGIC(NPs1mM), MAGIC(NPs2mM) and MAGIC(NPs5mM) gels properties using film 69
Fig.52. Comparison between X-ray absorption coefficient values in MAGIC(6%) and MAGIC(NPs2mM) gels 70

INTRODUCTION

In recent years gel dosimetry has expanded in the radiotherapy area. Gel dosimeters can be used as dosimeters as well as phantoms and in this way it could be verified three dimensionally (3D) dose distributions delivered to the cancer during radiotherapy treatment. These advantages could be applied on dosimetry evaluation where steep dose gradients exist such as in intensity-modulated radiation therapy (IMRT) and stereotactic radiosurgery. Gel dosimeters have also specific advantages in brachytherapy, applications of gel dosimeters also exist in low-energy X-ray, high-linear energy transfer (LET) and proton therapy, radionuclide and boron capture neutron therapy dosimetry. These 3D dosimeters are radiologically soft-tissue equivalent with properties that may be modified depending on the application [1].

Gel dosimetry is generally classified to Fricke and polymer gels [2]. Fricke gel dosimeters consist of ferrous sulphate (Fricke) aqueous solution incorporated into a gel matrix, due to such construction it is possible to stabilize the geometric dose information [3]. Polymer-type gel dosimeters are monomers dissolved in a gel matrix and these monomers get polymerized as a result of irradiation. The polymerization rate is proportional to absorbed radiation dose. The main polymer gel dosimeters are: Polymethacrylic Acid Dosimeters (methacrylic acid, gelatin, water, and small amounts of other agents (i.e., THPC or other oxygen scavengers)); Polyacrylamide Gel Dosimeters (use two monomers, acrylamide or another mono-vinyl monomer and bisacrylamide, a divinyl cross-linker which induces micro gel formation and precipitation) [3].

Nanotechnology is currently one of the most expanding fields of science. Nanotechnology can be successfully applied in polymer gel dosimetry. Metal nanoparticles, having the range from 1 to 100 nm, are inserted in polymer gel dosimeter matrix to enhance the dose deposited while using lower radiation dose as well as for better imaging purposes [2].

The polymer gel dosimetry is the three-dimensional dosimeter for extracting the dose, which can be used along with the nanoparticles for better therapeutic efficiency for modern radiotherapy techniques. Gel dosimeters with inserted nanoparticles could improve optimization of therapeutic or diagnostic dose. Sparing of healthy tissues and targeting the tumor part could be achieved with help of polymer gels with incorporated nanoparticle investigations. Gel dosimeters might be used as both phantom and dosimeter in one place. It is important to evaluate incorporated nanoparticles impact on ionizing radiation absorption in gel.

Object: Development and investigation of MAGIC gels of enhanced sensitivity to ionizing radiation by adding silver nanoparticles.

Tasks:

1. To analyze and evaluate polymer gels used in clinical environment, introduce their advantages and disadvantages.
2. To prepare MAGIC dosimetric gels with varied chemical composition and investigate influence of ionizing radiation on the physical characteristics of gels.
3. To Einvestigate silver nanoparticles produced by photoreduction method impact on dosimetric characteristics of MAGIC gels
4. To investigate X-ray absorption properties of gels modified by silver nanoparticles.

1. THEORETICAL REVIEW

1.1 IONIZING RADIATION IN THE MEDICINE

Nowadays ionizing radiation (IR) has widely applications in the field of medicine. Here is number of diagnostic and therapeutic procedures where the IR is used.

Diagnostic applications of ionizing radiation are basically divided in two areas: radiology and nuclear medicine [4]. In radiology the radiation exposure is external, while in nuclear medicine it is internal. The most conventional radiology procedures are: conventional radiography (chest, spine, pelvis, bones) X-ray mammography, computed tomography (CT). In the case of nuclear medicine the radionuclides or/and radiopharmateceuticals are injected to the patient. Depending on the metabolic pathways of the pharmaceutical in question and disease status of the patient to be studied, the radiopharmaceutical is distributed non-uniformly throughout the body. Gamma rays are emitted due to radionuclide decay and could be registered using detectors. In this way the contrast is improved and the observation of metabolic activity could be done. The most conventional nuclear medicine examinations are: SPECT and PET [4].

Radiation therapy is widely applied in the cancer treatment for all part of human body. Here are several techniques of radiation therapy which are recently applicable in medical facilities. External beam radiotherapy includes: conventional radiotherapy (fractionation), 3D conformal radiotherapy (3DCRT), intensity modulated radiation therapy (IMRT), image-guided radiotherapy (IGRT), stereotactic body radiation therapy (SBRT) [2]. In fractionation the total radiation dose for the tumor is delivered in relatively small fractions in order to let normal tissue cells repair damage caused by ionizing radiation. Typically fractionation consists of daily fractions of 1.5 to 3 Gy given over several weeks [2]. 3DCRT based on CT imaging which certain accuracy of localization of the tumor and sensitive organs hence the beam localization and shielding is optimized. IMRT allows create irregular-shaped radiation doses distribution that conform to the tumor whilst simultaneously avoiding critical organs [2]. IGRD allows evaluate organs motion during treatment, avoid unfounded healthy tissue irradiation and determine tumor localization [5]. SBRT technique precisely delivers very high individual doses of radiation over only a few treatment fractions to ablate small, well-defined primary and oligometastatic tumours anywhere in the body [5]. Brachytherapy is internal radiation therapy during which the small radioactive sources are implanted directly to the tumour [6]. These sources could be removed from the tissue or remain. Brachytherapy is classified by the dose rate: a dose rate of 40 to 200 cGy per hour (cGy/h) as a low dose rate (LDR), 200 to 1200 cGy/h as a moderate dose rate, and greater than 1200 cGy/h as a high dose rate (HDR) [6].

The summary of ionizing radiation application and parameters in medical procedures presented in table 1 and 2.

Table 1. Applications of IR in medicine [5]

Radiation source	Applications	
	Diagnostic	Therapeutic
Reactor-generated by product material	Nuclear medicine	Brachytherapy
Radium (Ra)	Nuclear medicine	Brachytherapy
Accelerator-generated radionuclides	Nuclear medicine	Brachytherapy
X-radiation	Radiography Fluoroscopy Computed tomography Dental X-rays	External beam X-ray therapy
High-energy particle radiation		Electron, neutron, positive ion therapy and Boron neutron capture therapy

Table 2. Main parameters of IR used in medical procedures [7-11]

Application	Dose range	Photon energy range
Medical: diagnostic	0.1 – 100 mGy	10-150 keV
Medical: therapeutic	1-10 Gy (per fraction) 45-80 Gy (in total)	0.5 – 50 MeV

1.2 INTERACTION OF RADIATION WITH MATTER

Ionizing radiation is radiation which has enough energy to excite atom and eject electrons from the atom of material with which it interact (create ions). The minimum energy needed to ionize an atom (to remove an electron from valence band) is in range of 4-25 eV (12.6 eV for water) [11, 13]. Radiations must carry kinetic or quantum energies in excess of this magnitude to be called "ionizing". The energy of photon could be calculated by [12]:

$$E=h\nu \quad (1)$$

here h- Planck's constant (6.626×10^{-34} J s) and ν is the frequency of electromagnetic wave.

There are two mechanisms through that radiation ionize atoms: direct ionization (fast charged particles that deposit their energy in matter directly, through many small Coulomb (electrostatic) interactions with orbital electrons along the particle track) and indirect ionization

(photons or neutrons that first transfer their energy to matter and create secondary charged particles which direct interact with matter) [13].

The main radiation interaction mechanisms through which radiation interacts with mater are photoelectric effect, pair production, Compton scattering and coherent scattering [14].

During coherent scattering photon interacts with atom and causes momentarily vibration of electron or atom. Vibration energy released as the photon with same energy and same frequency as incident photon, so no energy is absorbed in the matter. Only direction of incident photon changes it is scattered at small angle (Fig 1. A) [14]. The coherent scattering occurs in high-atomic-number materials and with photons of low energy.

In the Compton scattering incident photon interacts with "free" electron usually from valence band. In this case the electron binding energy is much lower than the energy of the incident bombarding photon. During this interaction electron absorbs part of the photon energy and is emitted at an angle θ. The photon energy is reduced and it is scattered at an angle φ (fig.1 D)) [14]. Essential condition for Compton scattering is that the energy of the incident photon must be large compared with the electron-binding energy. The Compton scattering decreases with increasing photon energy. Compton interaction involves essentially free electrons in the absorbing material hence it is independent of atomic number Z [14].

Photoelectric effect occurs then all incident photon energy is absorbed by the atomic electron and it is ejected from the atom. The kinetic energy of the ejected photoelectron is equal for incident photon energy and electron binding energy difference [14]. The vacancy created by ejected electron results atom excitation. The vacancy can be filled with the electron by an outer orbital electron with the emission of a characteristic X-ray (Fig.1. C) [14]. There is also the possibility of emission of Auger electrons, when the released photon energy is given to another electron in a higher shell, which is ejected afterwards. The probability of photoelectric effect increases when the energy of the incident photon is equal to or slightly greater than the binding energy of the electron in K, L, or M shell. Photoelectric effect depends strongly on the atomic number of the absorbing material, decrease approximately as Z^3 [14].

Pair production can be observed then the incident photon energy is higher than 1.02 MeV. During this process the incident photon interacts strongly with the electromagnetic field of an atomic nucleus and transfers all its energy to the atom. The pair of a negative electron (e^-) and a positive positron (e^+) is created (Fig.1. B)). The positron annihilates with an electron to create two 0.511 MeV photons, separated at an angle of 180^o [14]. Pair production process increases with increasing photon energy and increases with atomic number approximately as Z^2 [14].

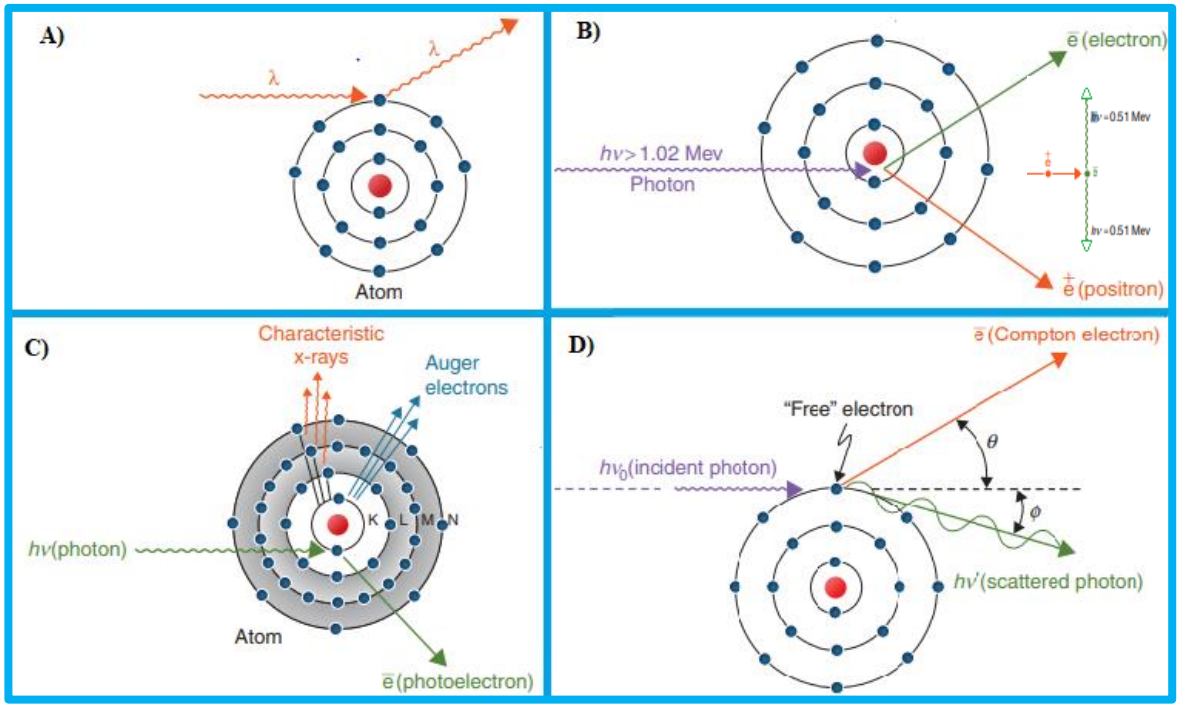

Fig. 1. Illustration of different radiation interaction with matter mechanisms [14].

1.3 RADIATION DOSIMETRY SYSTEMS

Radiation can damage biological tissue by changing cellular structure and damaging an organism's DNA. The amount of damage depends on a number of factors: most important from them are the type and quantity of radiation absorbed and its energy [15]. Consequently measurement of radiation quantity is very important task in radiation diagnostic, radiotherapy and radiation safety. The main parameters which describe radiation quantity are listed in table 3.

Table 3. Quantities used in radiation measurements [12, 16-18].

Radiation quantity	Description	Formula	Old units	SI units
Absorbed dose	Energy absorbed per unit mass of absorbing media (radiation concentration absorbed by patient)	$D=\frac{\Delta E}{\Delta m}$	rad	Gy
Equivalent dose	Absorbed dose multiplied by a radiation-weighting factor (biologic impact of radiation)	$H_T=\sum_R w_R D_{T,R}$	rem	Sv
Effective dose	Equivalent dose multiplied by tissue-weighting factor (organ-specific impact of radiation)	$E=\sum_T w_T H_T$	rem	Sv
KERMA	Kinetic energy released in matter defined for indirectly ionizing radiation and is related to the first step of transfer of energy from these particles to matter.	$K=\frac{\Delta E_{tr}}{\Delta m}$	Gy	Gy
Exposure	The ability of photons to ionize air is defined as charge of either sign produced per kilogram of air (radiation concentration present in field)	$X=\frac{\Delta Q}{\Delta m_{air}}$	R	C/kg (coulomb per kilogram)

where:

ΔE - is absorbed energy.

Δm - is the mass of medium.

w_R - is the radiation weighting factor.

w_t – is the tissue weighting factor.

ΔE_{tr} - is energy transferred from indirectly ionizing particles to charged particles in absorber.

ΔQ - is the charge of either sign collected.

Δm_{air} - is the mass of air.

Different types of dosimeters are used for radiation registration and quantification. Methods for detecting radiation are therefore essential for the successful operation of diagnostic imaging equipment, also to ensure reproducible operation of all such equipment and for the personal safety of staff and patients. The main types of radiation dosimeters used in medical field are: ionization chambers, calorimetric radiation detectors, solid state radiation detectors, radiation films and gel dosimeters [17].

In ionization chambers the energy deposited by the ionizing radiation produces ion pairs [16]. Usually ionization chambers are filled with gas and have two electrodes which is used to collect ion pairs. The voltage applied across the electrons should be high enough to ensure that all ion pairs produced by the incident photon are collected and low enough to avoid secondary ion production by the motion of the primary ion pairs [19]. Electrometer measures the small ionization charge produced in the radiation sensitive volume or the associated small ionization current [17].

Calorimetric dosimeters based on measurement of thermal (heat) energy transferred from a radiation to absorbing medium. This is most direct and fundamental measurement of the absorbed dose because if the absorbing medium is insulated from environment then the rise in temperature of the medium is proportional to energy absorbed from incident radiation [17].

Solid state radiation dosimetry has three main detector types: thermoluminescent, optically stimulated luminescence, scintillation and semiconductor [19]. In thermoluminescent dosimeters radiation sensitive material (LiF: Mg,Ti) trap the charge-formed ionization electron/hole pairs in metastable states within crystal [19]. The trap is impurities of the crystal. At room temperature majority of the electrons could not escape from the metastable state unless they gain additional energy. The additional energy is given by heating, when trapped electrons have enough energy to leave metastable state and back to the valance band and recombine. The energy released during this process mainly is in form of optical photons which could be detected by a photomultiplier (PM) and correlated to the absorbed dose received by the TL material [19].

In optically stimulated luminescence dosimeters (OSLs), instead of the heat for trapped electron release is used visible or ultraviolet light. The main material is carbon-doped aluminum oxide (Al_2O_3:C).

Scintillation detectors could be not only solid but also liquid. Here organic and inorganic solid state scintillators as well. Scintillators consist from crystal material in which incident radiation excites electrons and they rise to higher energy level state. These electrons could be trapped in crystal impurities like in OSLs and TLDs. Light is released then these electrons return to the ground energy state. Light photons are pointed to photosensitive cathode of a photomultiplier tube. Light photon ejects electrons from photocathode if the wavelength of light striking the photocathode matches the spectral sensitivity of this photosensitive surface. In photomultiplier tube these photoelectrons are multiplied and signal could be registered from the anode of the photomultiplier [17]. The main inorganic crystals used in scintillation is NaI(Ti), CsI(Ti) and KI(Ti) [20].

Semiconductor detectors are generally based on silicon (Si) and germanium (Ge) crystals. Nowadays other materials such as metal-oxide-semiconductor and diamond for semiconductor diodes are used [17]. The mechanism of semiconductor detector is similar with ionization chambers, except that sensitive volume in which electron-hole pair produced is not gaseous but

solid. The electron-hole pair produced in sensitive volume of the semiconductor dosimeters can be converted to a voltage pulse. These pulses could be registered with electrometer. Created amount of electron-hole pairs are moving in the electric field and then is collected at electrodes either side of the detector. The amount of charges collected is proportional to energy from radiation absorbed by medium. Crystal imperfections and impurities affect drastically the electronic properties of semiconductors. Here are two types of impurities in semiconductor crystal: donors (P, As, Sb) and acceptors (B, Al, Ga). Donors introduce occupied energy level into forbidden energy band gap right below the conduction band. In presence of these levels electron from them can be easily excited and rise to the conduction band. In donor type semiconductors are many more free electrons in the conduction band than free holes in the valence band and conduction occurs mainly by electrons in the conduction band [17]. Acceptors introduce vacant energy levels in the forbidden energy band gap right above the valence energy band. Electron exited from valence band can rise to these levels and, in this way, produce free holes in valance band. In acceptors type semiconductor are many more free holes in the valence band than free electrons in the conduction band and conduction occurs mainly by holes in the valence band [17].

Film radiation dosimetry is divided in two groups by type of the film: radiographic film and radiochromic film. The main difference between these films is readout technique: processing of radiographic film requires additional sophisticated developers and fixers, while radiochromic film is self-processing and no additional film processing is required. Recently radiochromic film is more used in dosimetry. Radiochromic and radiographic films consist from layers as shown in Fig.2. each of them have different function [17].

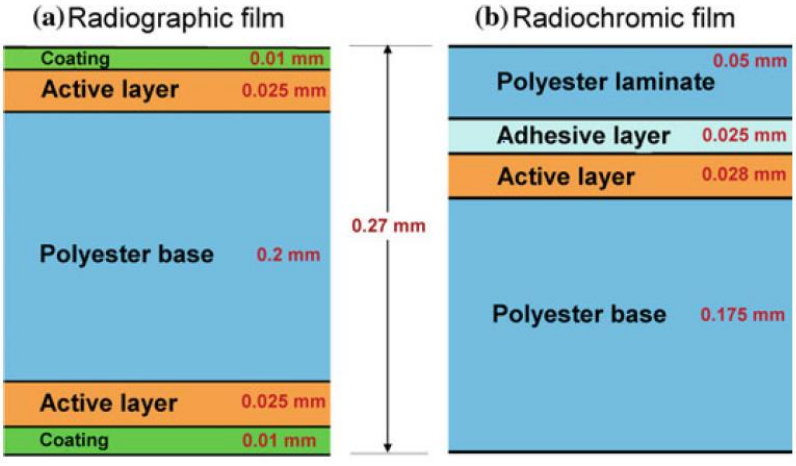

Fig.2. Structure of the different dosimetric films [17]

The most important layer of the film is the active layer/emulsion. This layer consists of imperfect silver halide crystals (~95% AgBr and ~5% AgI) suspended in gelling agent (usually gelatin) [17]. Size of grain varied from 0.2 to 10 μm [19]. During irradiation photon interacts

photoelectrically with the halide and the free electrons are released. Some of these electrons formatted in the conduction band of the AgBr crystal may get trapped in shallow electron trap. These trapped electrons interact with Ag^{+}, and formed metallic silver atoms. After film processing film grains containing more than a critical number of non-ionized silver atoms are then completely reduced to metallic silver [19]. Grains with less than this critical number are removed by the fixing process [19]. And in this way the latent image is formed. Radiochromic film is based on poly-diacetylene active layer. During irradiation these film change color by polymerization reaction [19]. Color change or film darkening is proportional to absorbed dose in film active layer and can be measured as dosimetric signal.

The main significant characteristics in dose registration, advantages and disadvantages of each dosimetry system are summarized in Table 4.

Table.4. Advantages and disadvantages of main radiation dosimeters [17-21].

Dosimeter	Advantages	Disadvantages
Ionization chambers	Energy range from 34keV to 35MeV; Suitable for absolute and relative radiation dosimetry; No readout required; Small size; Accurate and precise Recommended for beam calibration; Necessary corrections well understood; Instant readout;	High voltage supply required; Many corrections required for high energy beam dosimetry;
TLD and OSL	Small in size: point dose measurements possible; Many TLDs/OSLs can be exposed in a single exposure; Available in various forms; Some are reasonably tissue equivalent Not expensive; TLDs have useful dose from 0.5 μGy to 500 Gy;	Signal erased during readout; Easy to lose reading; No instant readout; Accurate results require care; Readout and calibration time consuming; Not recommended for beam calibration;
Scintillators	High sensitivity; Instant readout; Radiation damage (if organic); Small size; High output;	Temperature dependence; PM tubes require a high-voltage supply; Expensive;
Semiconductors	Small size; High sensitivity; Instant readout; Excellent energy resolution; linear response with deposited energy; Energy required to create charge 3 – 5 eV;	Variability of calibration with temperature; Change in sensitivity with accumulated dose; Special care needed to ensure constancy of response; No tissue equivalency;

Films	2-D spatial resolution; Very thin: does not perturb the beam; Film has an excellent spatial resolution;	Darkroom and processing facilities required; Processing difficult to control; Variation between films and batches; Needs proper calibration against ionization chamber measurements; Energy dependence problems; Cannot be used for beam calibration; Film is not useful for absolute dosimetry;
Calorimeters	Direct measuremen;t	Not practical for routine measurements; Required highly stable measurements condition; Difficult to measure extremely small temperature rises; Useful only for absolute dosimetry;

1.4 FRICKE DOSIMETRY

Gel dosimetry as well as the polymer gel dosimetry begins from Fricke dosimetry. In Fricke dosimetry system, the dose is determined by evaluating the chemical changes produced by radiation in the ferrous sulphate (Fricke) solution of the dosimeter [22]. Usually Fricke dosimeter consist of triply water, ferrous ion (usually from $FeSO_4(7H_2O)$ or $Fe(NH_4)_2(SO_4)_2(6H_2O)$), sulphuric acid (H_2SO_4), air or oxygen, and gel [23]. An important aspect of this dosimetry system is to stabilize the geometric dose localization by incorporating the aqueous Fricke solution into a gel matrix.

During irradiation ferrous ions (Fe^{2+}) are transformed into ferric ions (Fe^{3+}) and this transformation is dose dependent. When the solution is irradiated, water dissociation begins and hydrogen atoms start to interact with oxygen to produce the hydroperoxy radical [23]:

$$H^{\bullet} + O_2 \rightarrow HO_2^{\bullet} \qquad (2)$$

Ferrous ion oxidation into ferric ion could occur during different reactions [23]:

$$\begin{gathered} Fe^{2+} + OH^{\bullet} \rightarrow Fe^{3+} + OH^{-} \\ Fe^{2+} + HO_2^{\bullet} \rightarrow Fe^{3+} + HO_2^{-} \\ HO_2^{-} + H_3O^{+} \rightarrow H_2O_2 + H_2O \text{ and} \\ Fe^{2+} + H_2O_2 \rightarrow Fe^{3+} + OH^{\bullet} + HO^{-} \end{gathered} \qquad (3)$$

In order to confirm the existence of ferric ions and to make sure that the environment is changed to ferric, a metal ion indicator was used which turns light yellow in ferrous environment and then to dark brown in ferric environment [2]. The amount of produced Fe^{3+} depends of energy absorbed by dosimeter (solution). The ferric ion concentration changes estimate absorbed dose by [24]:

$$\Delta[Fe^{3+}] = \frac{D \cdot G(Fe^{3+}) \cdot 10\rho}{N_A \cdot e} \qquad (4)$$

here D is the dose, $G(Fe^{3+})$ is the chemical yield of Fe^{3+} (expressed in ions produced per 100 eV), ρ is the density in kg/l^{-1}, N_A is Avogadro's number and e is the number of Joules per electron volt [23]. The chemical yield of ferrous ion for well-prepared aqueous Fricke solution is 15.6 Fe^{3+}/100 eV [6]. In the Fricke gel system chemical ferrous ion yield is higher than in aqueous Fricke solution, because of additional Fe^{2+} transformation into Fe^{3+} provided by the gel macromolecules. From (4) equation the basis of Fricke and Fricke-gel dosimetry could be established: the dose absorbed by an irradiated Fricke dosimeter can be evaluated by measurement of the concentration change of Fe^{3+}.

1.4.1 Fricke gel preparation and composition

As was mentioned above the main component of Fricke gels are: water (it is important that water would be distilled or deionized), ferrous ion (usually from ferrous ammonium sulphate), gel and additives such as sulfuric acid, NaCl, air or oxygen. The ferrous ions are responsible for chemical changes induced by the radiation in sensitive dosimeter volume and the gel provides better spatial resolution of the radiation-induced changes (slow down movement of produced Fe^{3+} ions).

The Fricke gel began to produce by gel pouring to 75% of the water and heated until the gel has dissolved [23]. The other required regents are added to the remaining 15% of the water and this solution is mixed with gel solution. This compound for a short time kept at high temperature to ensure complete mixing. Prepared dosimetry gel usually stored at low temperature and in the dark environment to minimize chance of spontaneous conversation of Fe^{2+} to Fe^{3+} which perforce occurs.

Various gelling agents were used for gel dosimetry but agarose and gelatin are generally choice. Alternative such as agar, Sephadex and polyvinyl alcohol (PVA) have limited usage. Fricke gel dosimetric qualities depend critically on the gelling agent used in the preparation. Gelatin and agarose produce stable, well characterized dosimeters. Gelatin dissolves in water around 45°C, have good characteristics is comparative cheap so is mainly choice in gel preparation. Agarose dissolves

in water about 90°C in this connection gel matrix in agarose may degrade in larger degree in the acidic solution [25].

The chemical composition of the gel affects the ferric ion concentration changes and in this way influences the radiation chemical yield (table 5). Organic impurities can infuse new pathways for Fe^{2+} oxidation and the chemical yield increases. Sodium chloride NaCl was specifically incorporated into the traditional aqueous Fricke to help control the perturbation of the dose response by small amounts of organic impurity [3].

In the development of Fricke gels specific additives, or dopants, could be included in the gels, for example, to increase the dose sensitivity to enhance uniformity of gel preparation, and to provide mechanisms to enable optical examination of ferric ion conversion. Additives or dopants, such as benzoic acid have been included in the preparation of Fricke gels to increase the dose sensitivity. The justification for such doping was based on an increase in the dose response of the doped Fricke gels relative to standard aqueous Fricke rather than to the response of undoped gels [3].

Table 5. Some typical recipes with concentrations of main constituents for the most common Fricke and Fricke gel dosimeters with representative chemical yields [3].

Gel	gel (wt/wt %)	Fe^{2+}, mM	H_2SO_4, mM	NaCl, mM	$G(Fe^{3+})$ (Fe^{3+}/100eV)
Aqueous	0	1	0.05	1	15.6
Gelatin	4 10	1	0.05	1	45 43
Agarose	1 2	1	0.05	1	94 99
PVA	20	0.4			~20

Fricke gel (after irradiation) has the problem of ion diffusion by which it does not maintain a spatially stable distribution of dose [2]. For this reason the dose has to be extracted within 2 h after the irradiation of the gel. Chelators, organic chemicals that form two or more coordination bonds with a central ferrous or ferric ion are additives used to increase spatial resolution of gel. Appropriate chelators provide positive modifications for practical dosimetry: they improve the stability of the spatial dose information by reducing the diffusion coefficients of the iron ions [26]. Chelators, such as xylenol orange or glyoxal, significantly decrease diffusion, especially in gelatin Based Fricke dosimeters. The absorbed dose in range of 40-400 Gy can be measured using Fricke dosimeter [25].

.

1.5 POLYMER GEL DOSIMETRY

1.5.1 Chemical principles of polymer gel dosimetry

Polymer gels are mainly monomers dissolved in a gel matrix and after irradiation these monomers get polymerized. The rate of polymerization depends on the absorbed dose. The main constituent of the polymeric gel is water (about 90%) [1]. Ionising radiation passes through material and transfers part of its energy during various interactions. Absorbing material absorbs energy during irradiation and the components of material could decompose. When ionizing radiation passes through water, its molecules dissociate into several highly reactive species, this process is called radiolysis. Radicals and ions created during radiolysis could initiate secondary ionization [1].

Radiation chemistry mechanisms in polymer gel could be described by simplified reactions of which the dissociation rate ($k_{D)}$ is proportional to the absorbed dose [1]. The first stage is radiolysis [1]:

$$H_2O \xrightarrow{k_D} 2R^{\bullet} \qquad (5)$$

The radicals initiate polymerization of monomers by reacting with them. This step called initiation and can be written as follows with $k_I(n)$ the initiation reaction rate constant [1]:

$$R^{\bullet} + M \xrightarrow{k_I} M_I^{\bullet} \qquad (6)$$

The polymer growth continues by chain propagation reactions in which the monomer radical react with another monomer (or formed polymer chain with m monomers) and add them to the polymer chain. This is a determinant step where monomers react together, forming a polymer. The general way in which a polymer radical with m monomer units reacts with a monomer is shown in equation [1]:

$$M_m^{\bullet} + M_n \rightarrow M_{m+n}^{\bullet} \qquad (7)$$

The physical properties of the dosimeter changes in presence of this newly formed polymer and different techniques can be used to probe these changes. A calculation based on reasonable assumptions suggested the number of monomer units in a polymer chain was roughly 10^4 [27].

Termination of the gel polymerization is also an important reaction since an absence of termination would result in full polymerization of the monomers after a negligible radiation dose.

Polymerization reaction can be terminated by two polymer radicals react together, a polymer radical can react with water free radical or with gelatin. Termination could be written as follow [1]:

$$M_m^{\bullet} + M_n^{\bullet} \rightarrow M_{m+n}$$
$$R^{\bullet} + M_n^{\bullet} \rightarrow M_n \qquad (8)$$

The simplified scheme of the chemical reactions which occur in polymer gels during irradiation presented in Fig.3.

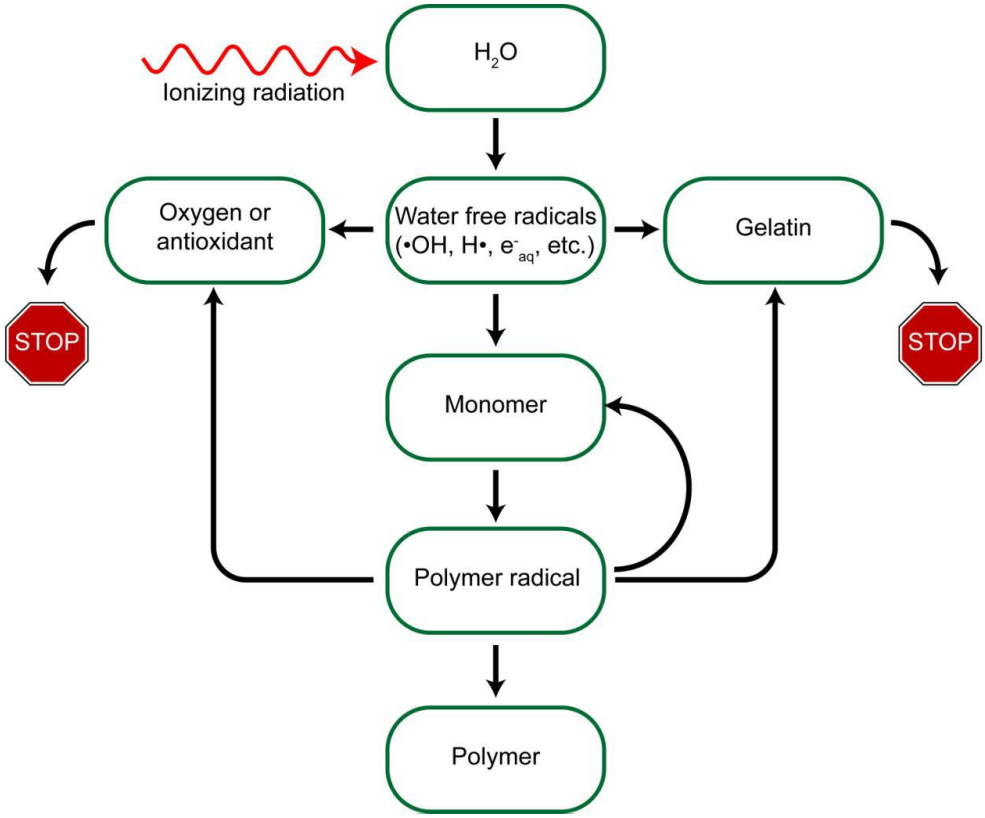

Fig.3. Schematic representation of photon interaction with dosimetric gels. [28].

The major problem in gel dosimetry is oxygen species which occur in gels. Oxygen is a very reactive chemical species so then oxygen is present in the gel that will rapidly react with monomer radicals or with water free radicals, efficiently terminating or inhibiting the polymerization reaction (Fig.3.). The main compounds which induce termination of the polymerization is peroxide-radicals, which are created when oxygen is present in the gel [1]:

$$R^{\bullet} + O_2 \rightarrow ROO^{\bullet}$$
$$M_n^{\bullet} + O_2 \rightarrow M_nOO^{\bullet} \qquad (9)$$

These peroxide radicals instantly react with other radicals in gel leading polymerization to termination [27]:

$$\begin{aligned} ROO^{\cdot} + R^{\cdot} &\rightarrow ROOR \\ ROO^{\cdot} + M_n^{\cdot} &\rightarrow ROOM_n \\ M_N OO^{\cdot} + R^{\cdot} &\rightarrow M_n OOR \\ M_n OO^{\cdot} + M_m^{\cdot} &\rightarrow M_n OOM_m \end{aligned} \qquad (10)$$

This problem is solving in two different methods: preparing the dosimeter gel in an oxygen-free environment (such as nitrogen-purged glove-box) or (and) an antioxidant is added to the gel composition, which scavenged oxygen molecules present in the gel during gel formation under normal atmosphere conditions.

The first method is used for several years by bubbling nitrogen through the gel solutions and by filling the phantoms in a glove box that is perfused with nitrogen [28]. Critical importance has housing of the gels since even minute oxygen contamination can alter the gels responsivity, linearity and reproducibility. Thus, the gels are typically contained within glass vessels which have lower permeability to gas but are also less tissue equivalent and less readily formed than plastic containers [28].

In this research the second method is more acceptable, because of its accessibility and simplicity. In this method the antioxidants (oxygen scavenger) are added to gel composition. The oxygen is bound in a metallo-organic complex in this gel thus removing the problem of oxygen induced termination (inhibition) of radiation-induced polymerization.

Y. A Deene et al. (2002) investigated different antioxidant effect on polymer gels [28]. In this research 5 antioxidants with different concentration were analyzed: ascorbic acid, gallic acid, trolox, N-acetyl-cysteine and tetrakis (hydroxymethyl) phosphonium chloride (THP). From the five anti-oxidants that were investigated, only three were found capable of successfully scavenging oxygen after a time period of five days. These were: ascorbic acid, N-acetyl-cysteine and tetrakis (hydroxymethyl)phosphonium (THP) [28]. This is mane oxygen scavengers used in normoxic (gels manufactured in normal room atmosphere) gels. Each of them would be discussed below.

Ascorbic acid. In gel systems where the ascorbic acid as the anti-oxidant is used are two man components: a chelate of copper and ascorbic acid. As was mentioned before oxygen is bound in a metallo-organic complex, in this case a complex consisting of the three components: ascorbic acid (AscA), copper (Cu) and oxygen (O_2) is formed in the presence of oxygen [28]. The oxidation of ascorbic acid is catalyzed in the presence of copper [30]. As copper – ascorbate complex is formed the free oxygen is attached to this complex and formed a new one [28]:

$$AscA + O_2 + Cu^{2+} \leftrightarrow AscA\text{-}O_2\text{-}Cu\text{ -Complex} \quad (11)$$

N-acetyl-cysteine. N-acetyl-cysteine needs more time to scavenge oxygen in comparision with AscA. The difference is presented in Fig.4 (a and b) [28]. For *N*-acetyl-cysteine (Fig4(b)), a dose threshold is present for concentrations lower than 10 mM for a sample irradiated five days post-manufacture [28]. It is expectation that the dose threshold will occur at lower concentrations after longer time.

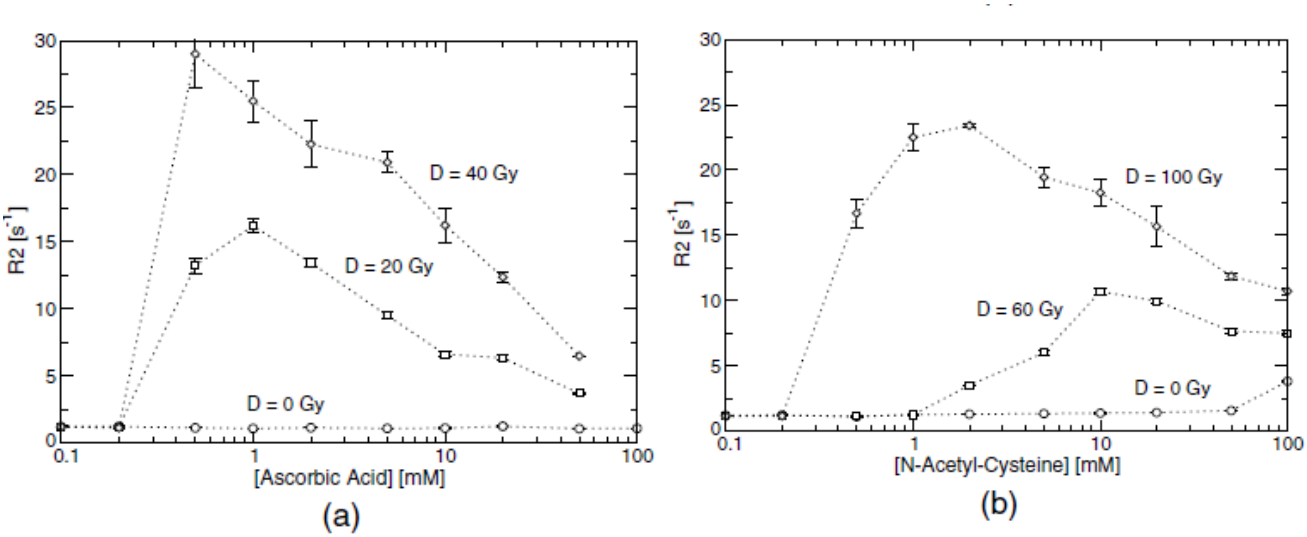

Fig.4. R2 for MAGAS gels containing different concentrations of ascorbic acid (a) and *N*-acetyl-cysteine (b). R2 plots are for gels that are irradiated five days after fabrication to three different doses [28].

Tetrakis (hydroxymethyl)phosphonium chloride (THP). THP has very high oxygen scavenging efficiency as well as it scavenge other free radicals, thus having an influence on other properties of the polymeric gel system and hence on the response of the dosimeter. The R2–dose response with THP was higher than with the $CuSO_4 \cdot 5H2O$, ascorbic acid, hydroquinone mixture [28]. It was also detected that $R2_0$ increased with increasing THP concentration once the threshold concentration was exceeded. Both these observations indicated, that THP not only act as a oxygen scavenger, THP also has ability to act as a promotor of the polymerization reaction. It was also determined that after a critical concentration the amount of THP has an influence upon the reaction rate but to a lesser extent on the resulting anti-oxidizing power [28]

Another research for THP influence on polymeric gel was made by V. Spěváček et al. (2014) [28]. In this investigation was found out that: increasing concentrations of THP, there is a decrease of both the R2 value and absorbance, while the linear part of dependence is lengthened. Evidently, the linear relationship between these quantities is valid for gels with THP in the whole examined range of the tested doses (i.e. up to 30 Gy). For gels without THP, the dependence is approximately linear

up to 12 Gy [31]. These findings are illustrated in Fig. 5. All in all THP was found to have the highest reaction rate. THP has not only ability to scavenge oxygen it also increases the dose sensitivity of the gel.

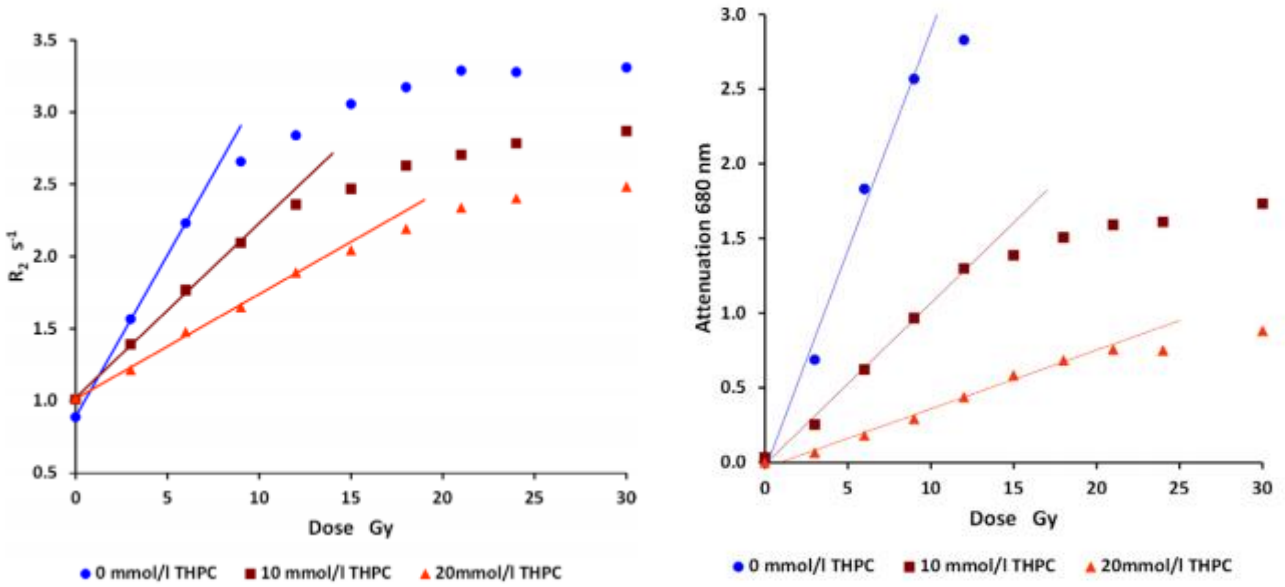

Fig.5. The dependence of R2 and of optical attenuation on dose for gels with different THPC concentration [31].

1.5.2 Polymer gels fabrication and composition

Polymer gel dosimeters consist of five mainly components: gelling agent (gelatin, agarose, PVA), monomer, catalyst and oxygen scavenger [32].

Agarose gels are made at temperature near 70°C, in this conditions the heat reduces the amount of dissolved oxygen and increases auto-oxidation rates. Such changes could produce chemically nonuniform gels with unnecessarily elevated background levels for optical studies [28].

Polyvinyl alcohol (PVA) has also been investigated as a gelling agent. PVA was investigated as a gelling agent due to the high purity, chemical simplicity, relative chemical inertness [11]. The high viscosity of PVA gels was problematic for preparation of large volume samples. Air bubbles became easily trapped when handling and became sources of nonuniformities, especially for optical readout. The scatter coefficients were also higher than analogous gelatin gels and continued to increase as the samples aged. For these reasons PVA gels have not been used for 3D dosimetry, but are quite helpful for investigating radiochemistries in hydrogels [28].

Gelatin is currently the most common gelling agent for manufacture radiosensitive hydrogels. The gelatin concentration is generally about 5% by mass (4-8%) [28]. Most common type of gelatin for hydrogels has been porcine, acid cured with a Bloom strength of 300 [28]. This gelatin type forms the tightest gels. Depending on the formulation, gelatin gels typically melt

between 28 and 34°C. In practice, if the gels are being handled in order to perform an irradiation experiment or transport to a readout instrument, temperatures exceeding 23°C may influence the gel uniformity [28]. Increased gelatin levels result in lower polymerization rates in all types of polymer gel dosimeters and to higher dose levels at saturation [33]. Higher gelatin concentration in gel system lead to higher values of R2 at zero dose, because higher gelatin leads to stiffer gels. Gelatin consumes long-lived radicals for this reason higher gelatin concentrations are associated with improvements in temporal and spatial stability of polymeric gels [33]. In gelatin based polymeric gels better optical and mechanical properties could be achieved.

Polymer gels are dosimeters in which the monomer is dissolved in gelling agent matrix. During irradiation the free radicals in water are produced these radicals induce the polymerization of the monomers, such that monomers are converted to polymers. The polymerization rate is proportional to absorbed radiation dose. The point of the gel matrix is to hold polymers in places hence the spatial information of absorbed dose is sustained. As was mentioned above the oxygen level in polymer preparation should be maintained as low as possible. Oxygen concentration in the polymer gel dosimeters had to be reduced to less than 0.01 mg l^{-1}, a factor of approximately 1000 lower than normal atmospheric conditions [1]. The quality of gel could be also effected by temperature during preparation and storage.

The perfect polymeric gel should be characterized by these features [1]:

- stability in space and time
- tissue equivalency
- dose rate and energy independent with the effect of temperature and pressure on the gel negligible

The number of different monomers is used in the polymer gel formation: acrylamide, acrylic acid, methacrylic acid, 1-vinyl-2-pyrrolidinone, 2-hydroxyethyl methacrylate and 2-hydroxyethyl acrylate. *N*,*N*-methylenebis- acrylamide was used as a co-monomer in each polymer gel dosimeter [34]. The structural formulas of main monomers are presented in Fig. 6 [34].

The polymer gels classified in two general types by the monomers used in gel formation. Additional if polymeric gel is prepared in normal atmosphere condition, such gels are called normoxic gel. Gels in which the main polymer is methacrylic are called MAGAT/nMAG and gels with acrylamide are called PAGAT/nPAG [32]. Here could be subtypes of each gel according the different chemical agents used in gel formation. The summarized list of polymer gel dosimeters is shown inTable 6 [32].

Table 6. Summary of polymer gel dosimeters (BIS - N,N'-methylene-bis-acrylamide, THPC: Tetrakis (hydroxymethyl) phosphonium chloride; THPS: Tetrakis (hydroxymethyl) phosphonium sulfate NIPAM: N-isopropylacrylamide; VIPAR: N-vinylpyrrolidone argon; HEA: 2-hydroxyethylacrylate; HEMA: 2-hydroxyethyl methacrylate; TGMEMA: Triethylene glycol monoethyl ethermonomethacrylate; 9G: Polyethylene glycol 400 dimethacrylate; SDS: Sodium dodecyl sulfate.) [32].

Dosimeter name	Type	Gelling agent	Monomer	Croslinker	Catalyzer/ stabilizer	Scavenger/ antioxidant
BANANA	PAG	Agarose	Acrylamide	BIS		Nitrous oxide
BANG	PAG	Gelatin	Acrylamide	BIS	Ammoniumpersulphate, TEMED	
BANG-2	MAG	Gelatin	Methacrylic acid	BIS	Sodium Hydroxide	AscA
BANG-3	MAG	Gelatin	Methacrylic acid		$CuSO_4 \cdot 5H_2O$	AscA
MAGIC	MAG	Gelatin	Methacrylic acid		$CuSO_4 \cdot 5H_2O$ Hydroquinone	
MAGAT	MAG	Gelatin	Methacrylic acid			THPC
nPAG	PAG	Gelatin	Acrylamide	BIS		THPS
nMAG	MAG	Gelatin	Methacrylic acid			THPS
nMAG	MAG	Gelatin	Methacrylic acid			THP
MAGIC-f	MAG	Gelatin	Methacrylic acid	Formaldehyde	$CuSO_4 \cdot 5H_2O$	AscA
HEA		Gelatin	HEA	BIS		
VIPAR		Gelatin	VIPAR	BIS		
NIPAM		Gelatin	NIPAM	BIS		THPC
PAG	PAG	Gelatin	Acrylamide	BIS	NaI	THPC
nMAG	MAG	Gelatin, Agarose	Methacrylic acid			THPC
nMAG	MAG	Gelatin	HEMA, TGMEMA, 9G			THPC

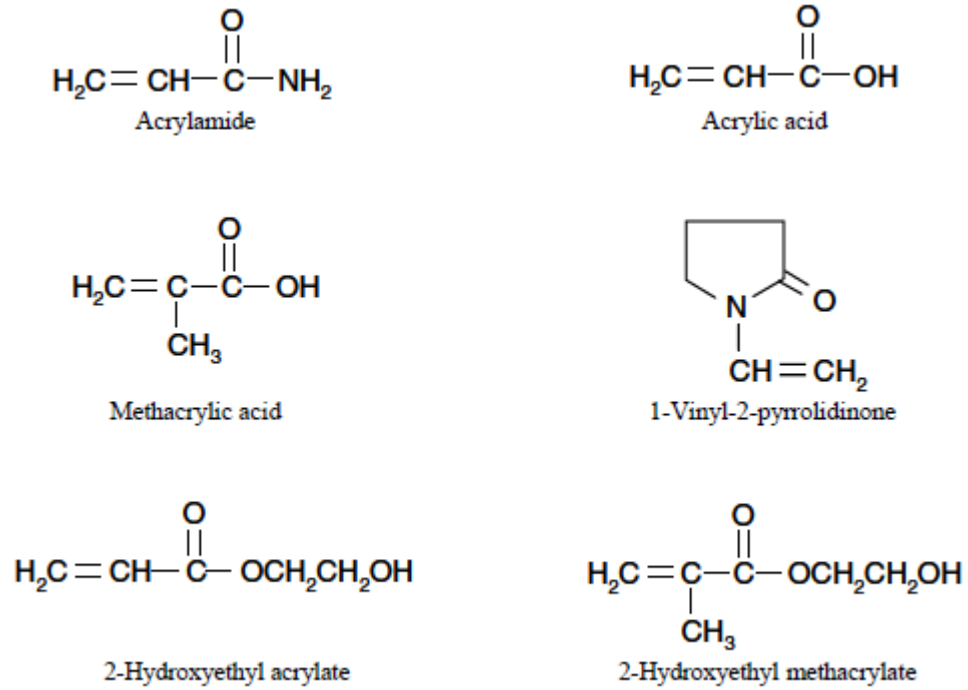

Fig.6. Chemical structures of different monomers used in polymer gel formation [34]

PAG dosimeters

Polyacrylamide-based gel (PAG) dosimeters are used in radiation dosimetry since 1990 [35]. In typical PAG dosimeters, gel is prepared of acrylamide, N,N'-methylene bisacrylamide, gelatin and water and then irradiated with dose from the range of interest. Unlike MAG dosimeters, PAG dosimeters, and the other dosimeters of this subtype (Table 6), use two monomers, acrylamide or another mono-vinyl monomer and bisacrylamide, a divinyl cross-linker which induces micro gel formation and precipitation [33].

Polymer chains grow during propagation reactions both acrylamide (which has one vinyl group) and bisacrylamide (which has two vinyl groups) are involved. Bisacrylamide tends to be consumed relatively more quickly than acrylamide because of the extra vinyl group [36]. When bisacrylamide is consumed by propagation, a pendant vinyl group (also called a pendant double bond) is created along the polymer chain. This vinyl group can subsequently react with a growing polymer chain to form a cross-link [36]. As polymer chains grow and cross-link, they become insoluble and deposit from the solution. The amount of polymer that precipitates and the cross-link density of the polymer chains influence water molecules that are dissolved within the precipitated polymer phase. As a result, the polymer deposition, and the radiation dose that produced it, can be detected using NMR or magnetic resonance imaging [36].

Several difficulties, which limit PAG dosimeters use for clinical application and radiation dosimetry exist [36]:

- long-lived radicals. In polymerization systems where branching, precipitation or cross-linking not occur , growing polymer molecules slightly diffuse through the reaction medium, react with other free radicals, and terminate. PAG dosimeters and other systems in which immobile cross-linked polymer molecules form, reduced growing polymer chain and other radicals diffusion this leads to slower termination reactions and higher polymerization rates. However reduced mobility of gel constituents result in continued polymerization after irradiation desist.To avoid the post-irradiation polymerization it is important to used well controlled sample handling techniques [36].
- edge enhancement, additional polymer forms near the edge of zones where the radiation dose is high. Mathematical simulations by K. B. McAuley (2004) were done to investigate this process. Simualtions indicate that almost no polymer forms beyond the edge of the irradiated zone, due to the very limited ability of the polymer to diffuse. However, essential amounts of extra polymer form just inside of the edge of the irradiated zone, due to diffusion and subsequent reaction of acrylamide and bisacrylamide molecules that were originally in the non-irradiated zone [36]. The amount of abundance polymer near the edge increases with increasing absorbed dose, using a fixed dose an also increases as the time post-irradiation increases. These additional polymers will result in incorrect information about the radiation dose that was applied near the edge. In order to reduce edge enhancement the larger monomer and cross-linker molecules that will diffuse less freely through the gelatin and water solution during irradiation should be used.
- monomer toxicity. The most limiting factor for PAG usage in clinical approach is the toxicity of acrylamide. Acrylamide is strong neurotoxin, also it is possible that acrylamide is carcinogen and a teratogen. It is easily absorbed by human through the skin as wel as through the respiratory tract. Bisacrylamide is less dangerous than acrylamide, because its molecules are bigger so it is more complicated to be absorbed by the skin or inhaled, nevertheless bisacrylamide is a suspected mutagen and teratogen. After acrylamide and bisacrylamide are polymerized, the polymer is safe to storage and use, as long as there is no remaining unreacted monomer. As is noted polymer gel dosimetry principle is to polymerize and cross-link acrylamide and bisacrylamide where the high radiation dose was absorbed, and leave them as unreacted monomers in zones where there is not affect by irradiation. So PAG dosimeters always consist of substantial amounts of unreacted monomers and are dangerous products. Nowadays it is attempting to replace acrylamide with othes, less toxic polymers such as N-vinyl formamide.

MAG dosimeters

Typical MAG dosimeter consists of methacrylic acid, gelatin, water, and small amounts of other agents (table 6). During radiation-induced water radiolysis formed radicals consumes metacrylic acid as monomer in polymerization, formed polymers precipitates and is held in place by the gelatin [33]. Polymethacrylic acid precipitates without the involvement of a cross-linker such as bisacrylamide, so methacrylic based dosimeters the croslinker is not required. MAG dosimeters also are less toxic than PAG so it is easier to handle and more suitable for clinical approach. However the study by Y De Deene et all (2006) was made in order to compare PAG and MAG suitability for dosimetry (it should be noted that only normoxic gels properties was investigated nMAG and nPAG) [37]. The authors found that the nMAG gel was superior in terms of dose sensitivity and stability over time while nPAG performed better in other areas. As was mentioned above the one of the main properties for the dosimeter is tissue equivalency, so MAG dosimeters have better tissue equivalency in comparison with other dosimeters type, it illustrate table 7 [29,38,39,].

Table. 7. Mass density, electron density, for MAG, PAG, MAGIC gels, water, human muscle tissue, bone, lung and fat [29,38, 39].

Material	mass density (g/cm^3)	electron density relative to water
MAG	1.046-1.05	1.044
PAG	1.035- 1.042	1.031
MAGIC	1.027-1.060	1.05
Water	1	1.0
Muscle	1.04	1.0328
Fat	0.916	0.9132
Bone	1.40	1.3492
Lung	0.296	0.293

MAGIC, the subtype of MAG dosimeters would be discussed more in details, because it will be used in this research.

MAGIC (methacrylic and ascorbic acid in gelatin initiated by copper) was proposed by Fong et al (2001) [29]. The main components of MAGIC gel are methacrylic acid, ascorbic acid, hydroquinone, cooper sulfate and deionized water. The methacrylic acid is as the monomer. It polymerizes upon irradiation. The ascorbic acid is a free oxygen scavenger with the higher efficiency. It is binding the oxygen in metalo-organic complex. The copper (II) sulfate is takes places as a catalyst in the oxidation of ascorbic acid. The gelatin holds polymer in place. Hydroquinone prevents instantaneous polymerization. Deionized water contains mobile protons. The bivalent complex of Cu^{2+} with ascorbic acid with molecular oxygen serves as a free radical sources, which initiates the polymerization of methacrylic acid. This complex allows the transferring of the electron to external species, thus generating free radicals that may initiate

polymerization. The ratio of O/C of MAGIC gel is 10.68. It is the much closer to the typical soft tissue (4.95). The mass density of MAGIC gels is 1060 kg/m^3. The mass density of MAGIC gels is higher in comparison with water by factor 1.06. It is more relative to mass density of human muscle tissue. The difference is 1.03. The difference factor of average atomic number of MAGIC and human muscle tissue is (7.07/6.93 =1.01). The difference factor of the electron densities of MAGIC and human muscle tissue is ($\frac{3.51 \cdot 10^{29} m^{-1}}{3.54 \cdot 10^{29} m^{-1}} = 1.03$). MAGIC is very attractive gel dosimeter because of its easy fabrication, good tissue equivalency, dose sensitivity, storage simplicity.

1.5.3 Dose evaluation in polymer gel dosimeters

The dose evaluation of an irradiated gel can be perform using different imaging techniques based on the specific physical change that has taken place in the irradiated gel. The three most commonly used imaging techniques for polymer gel dosimetry are MRI, optical-CT and X-ray CT [1].

Principle of MRI imaging is similar with Fricke gel dosimeters. Polymer gel dosimeters are based on the conversion of co-monomers to polymer induced by irradiation. This reaction shanges the mobility of surrounding water molecules which also results in a change in R1 and R2 (R1: the spin-lattice relaxation rate (R1 = 1/T_1); R2: the spin-spin relaxation rate (R2 = 1/T_2)). The dose-response of R2 in gelatin based polymer gel dosimeters however is more pronounced than of R1. Upon irradiation 3 pools of protons could be observed in the polymer gel [1]:

- the proton pool of free and quasi-free protons (denoted as mobile, *mob*). These are the protons from free water molecules and unreacted monomers;
- the proton pool of a growing polymer network (poly) and of water molecules bound to the macromolecules
- the proton pool of the gelatin matrix (gela) and of the water molecules associated with the gelatin.

The relaxation rate of the proton pools is inversely correlated with the mobility of the protons within these pools. In no irradiated bulk of polymer gel dosimeter the second proton pool is empty while the first proton pool is at its maximum. During irradiation the second proton pool starts to increase proportionally first pool of proton decrease. Upon irradiation of the gel dosimeters, the molecular mobility is significantly reduced. As the mobility of the bound water molecules is reduced, spin–spin relaxation is more effective, which is observed by an increase in *R*2. Alternatively, exchange of water protons with fast relaxing polymer protons will increase *R*2 [1].

After irradiation the irradiated regions of the polymer gel become visibly opaque with respect to absorbed dose. So optical dose evaluation methods, such as spectrometry, and optical CT are also available. Optical CT is similar to ordinary CT except using visible light instead of X-rays.

Measurements of the refractive index of gels irradiated to different doses revealed increasing refractive index with increasing dose [1]. The principle of optical CT is that the raw data are optical projections obtained either by a laser scanning across the sample, detected by a photoreceiver, or by broad incoherent light beam passing through the sample and imaged using detector. With reference to Beer's law, the measured signal intensity I could be related to the signal in the absence of the sample I_0 by [1]:

$$I=I_0\exp\left[-\int_{\text{ray-path}}\mu(s)ds\right] \tag{11}$$

where μ is the optical attenuation coefficient and *s* is a distance along the selected ray-path through the sample. μ changes are proportional to absorbed dose, so to evaluate the absorbed dose of the dosimeter we μ should be calculated from received mesurements.

During irradiation small changes in polymer gel dosimeter linear attenuation coefficient occurs, hence the X-ray CT could be used for dose evaluation. CT images are expressed as CT numbers (N_{CT}), in Hounsfield units (H). N_{CT} are measures of the linear attenuation coefficient of the sample (μ) relative to that of water (μ_w) [1]:

$$N_{CT}=1000\,\frac{\mu-\mu_w}{\mu_w} \tag{12}$$

Theoretically only density affects μ (and therefore N_{CT}). Therefore changes in irradiated gel density (ΔN_{CT}) are directly proportional to a change in gel density ($\Delta\rho_{gel}$) [1]:

$$\Delta\rho_{gel}=K\,\Delta N_{CT} \tag{13}$$

here *K* is a function of un-irradiated gel density. ΔN_{CT} in H is numerically equivalent to gel density change in kg/m^{-3}.

The change in density and viscosity in irradiated polymer gels also results in a change in speed of sound, so ultrasound also can be used for dose evaluation.

1.5.4 Applications of polymer gel dosimetry

Gel dosimetry is widely used in radiation therapy, radiation diagnostic and quality assurance because of the ability to measure 3D dose distribution and high spatial resolution. Gel dosimeters are dosimeter and phantom in one place, so that enhances possibilities of the gel dosimetry application. Part of polymer gel dosimetry application in radiotheraphy techniques schematic presented in Fig. 7 [2].

Fig.7. Radiotheraphy techniques where polymer gel dosimetry is applied [2].

Basic dosimetry. Gel dosimetry has the ability to display 3D dose distribution in the bulk of dosimeter. This is essential advantage over conventional dosimeters even in basic dosimetry measurements such as percent depth dose in photon and electron beams [40]. Dosimetry is effective in simple multiple-field arrangements validation and more complex anatomical situations including tangential breast treatment, conformal therapy and scalp treatment with electron beams as well [41-43]. Gel dosimetry has great success on dose evaluation in CT imaging because the dose distribution throughout a patient volume can be estimated without requiring the use of numerous point dosimeters (TLD) and without averaging the dose along a line or throughout a volume (pencil ionization chamber) [40].

3D CRT: 3D Conformal Radiation Therapy. SRS: stereotactic radiosurgery and SRT: stereotactic radiotherapy. Gel dosimeters shows good qualities for stereotactic therapy dose distribution display. Major benefit of gel dosimeters in stereotactic therapy and surgery is that they

display a dose distribution qualitatively in three dimensions without need of imaging systems or processing as it determined in Fig. 8 [40].

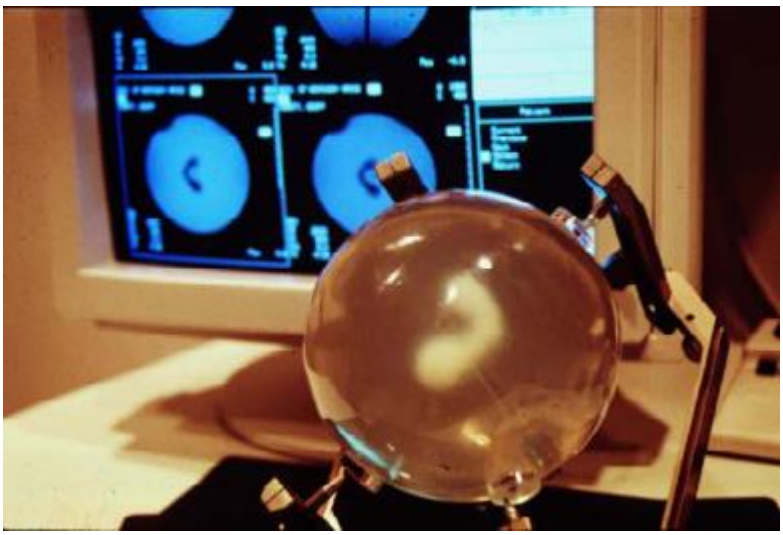

Fig.8. Human head gel phantom (BANG) irradiated with Gammaknife treatment unit dose distribution [40].

IMRT: Intensity modulated radiotherapy. Gel dosimeters are reliable in evaluating and confirming IMRT dose distribution. Dose distribution during IMRT was evaluated with both - simple geometric phantoms and anthropomorphic phantoms in arrangements that allowed direct comparison with measurements using other techniques such as film and TLD [43]. Measurements performed with an anthropomorphic head-and-neck phantom irradiated using IMRT showed that a polymer gel imaged with optical CT was reproducible to within 1% [40].

Brachytherapy. Determination of dose distribution and the results of planning confirmation for brachytherapy treatment is really difficult task, because it uses the small size of the radioactive material as radiation sources for radiation therapy inserted in patient body [32]. The ability of gels to record and display dose distributions around a high-dose rate (HDR) source based on capability to immerse the applicator containing the sources into the gel or arrange for its introduction into a catheter already placed in the gel. However, here are some issues for gel dosimeters application in brachytheraphy: significant dose deviations near the catheter wall, oxygen diffusion through the wall of the cavity may contaminate the gel and result in an underestimation of absorbed dose, energy dependence at lower energies in LDR brachytherapy, polymer gel dosimeter under-responds to radiation in the 20 keV – 60 keV range [1].

BNCT: boron neutron capture therapy. During BNTC tumor and surrounding tissues are irradiated with epithermal neutrons some gamma-radiation (480 keV) is released. Gel dosimeters s could be used to determine the profiles of neutron beams used for boron neutron capture therapy.

Some benefits of the use of gel dosimetry are the tissue-equivalence of the dosimeter to these energies, and the ability to separate the components of dose [40]. Also gel dosimeters could show the dose which affect normal tissue.

Tissue heterogeneity. Very beneficial feature of gel dosimeters is that they have high tissue-equivalency, particularly at photon beam energies above about 100 kV [40]. For this reason, gel dosimeters might be used to verify tissue inhomogeneities effect on dose distribution. With gel dosimeters the effects of non-unit density tissues on external beam dose distributions can be measured. The estimation tissue heterogeneity was performing for both: high atomic number heterogeneities, to simulate the presence of bone and cavities filled with air or with lung-equivalent plastic to simulate the presence of lung tissue [40].

Proton/heavy ions therapy. Polymer gel dosimeters can be used to record the dose distributions produced by proton beams. The measurement of the depth dose of particle beams, is an important task. However, the disagreements between measurements with gels and conventional dosimeters such as diodes in the peak region of the distribution were noticed [40]. As the LET of the beam increases in the peak region, the local ionization density increases. As the distance between the radicals formed in the gel decreases, the likelihood of recombination of radicals increases [40].

Diagnostic dosimetry. Polymer gel dosimetrers can be used in quality assurance of diagnostic CT scanners with respect to the exposure of patient dose [1]. The most important parameters that can be measured with a polymer gel dosimetry are the computed tomography dose index (CTDI) and the slice width dose profile (SWDP). The SWDP cannot be measured by an ionization chamber but is usually measured with either thermoluminescent dosimetry (TLD) or film. Gel dosimetry enables the registration of the whole 3D dose distribution and can be performed in an anthropomorphic phantom [1].

1.6 GEL DOSIMETERS AND NANOTECHNOLOGY

In recent years, the effect of high atomic number (Z) materials usage in radiotherapy has been studied. The role of metal nanoparticles (NP) is dose enhancement in tumor volume due to enhancing tumor radio-sensitivity by increasing the cross-section of radiation interaction in the tissue [44].

Enhancement of the radiation dose, which is performed by metal nanoparticles, appears in several ways. When radiation hits the target (tumor with nanoparticles) there are many possible interaction mechanisms illustrated in Fig 9 [45].

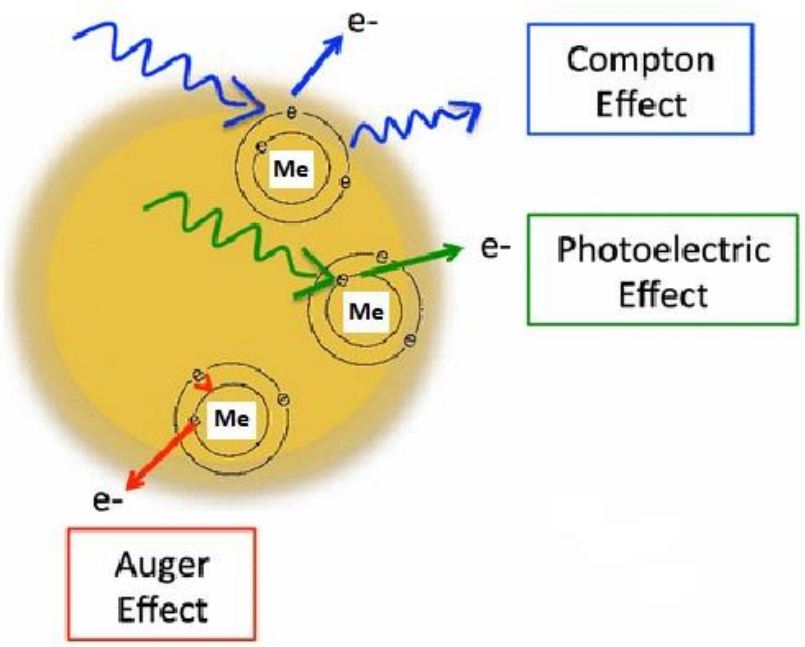

Fig.9. Schematic illustration of radiation interaction processes with nanoparticles [45]

The main physical mechanisms through which radiation interacts with nanoparticles in the keV range are the Compton and Photoelectric effects [45]. During Compton interaction (Fig. 9. blue), an incident photon is partially absorbed by outer layer electron and the energy is shared between the ejected (Compton) electron and scattered photon [46]. Photoelectric effect appears (Fig 9. green) when an incident photon interact with an inner orbital electron and transfer all its energy to the electron and the electron is ejected from inner atom electron layer. The kinetic energy of the ejected electron will be equivalent to the energy of the wave minus the binding energy of the electron [1]. The vacancy in the inner atom layer can be filled with electron from higher energetic layer and the surplus of energy is released as low-energy photon. These low-energy photons release secondary electrons (Fig.9. red), called Auger electrons. Auger electrons

have shorter ranges and can create higher ionization density at a localized area [1]. All these events occurring in the tumor volume enhance the radiation dose.

The dose enhancement with nanoparticles could be evaluated using polymer gel dosimeters because of it specific qualities such as tissue equivalency, 3D dose distribution evaluation, eassy usage and unsophisticated readout techniques. Condition of radiotherapy treatment can be simulated incorporating metal NP to tissue equivalent dosimeter.

Several researches have been performed recently for NP induced dose enhancement evaluation using polymer gel dosimeters [44, 47-49].

M. Hussan et al. (2016) accomplished research were the dose enhancement, using silver NP were investigated [25]. During this study the silver NPs were incorporated in MAGICA gel and enhancement was measured. The dose enhancement factor (DEF) was calculated in order to evaluate silver NPs effect for dose. The $AgNO_3$ concentrations of 0.05 mM and 0.10 mM were used in this study. The samples were irradiated with 5 Gy and 10 Gy radiation doses. After irradiation dose DEF was calculated for all samples. The results shows that with 0.05 mM AgNP concentration the DEF was 24.17 % and 40.49 % for 5 Gy and 10 Gy dose respectively and with 0.10 mM AgNP concentration DEF was was 32.88 % and 51.98 % for 5 Gy and 10 Gy dose respectively [44].

E. J. Jabaseelan Samuel et al. (2017) presented their investigation on dose enhancement of gold nanoparticle on different polymer gel dosimeters [48]. In this research ten different polymer dosimeters were used and dose enhancement produced by AuNPs was evaluated. AuNPs concentration was 7mgAu/g and the wide energy range (15 keV to 20 MeV) was used. Here also was calculated DEF. The result showed that maximum DEF was observed at 40 keV, while it was almost negligible at higher energy range. Dose enhancement produced by AuNPs on the gel dosimeter medium was varied compared to the reference ICRU-44 tissue, it was ± <1% for PAGAT, NIPAM, nPAG and ± <5% for PABIG, VIPAR, HEAG, BANG1, nMAG & ± <10% for MAGIC [48].

H. Khosravi et al. (2016) made study on AuNPs effect on the dose enhancement in the external radiotherapy [47]. In this investigation MAGICA polymer gel dosimeter was used, incorporated with 0.02mM, 0.05mM and 0.1mM AuNPs concentration. The 18 MV photon beams were used to simulate external radiotherapy treatment the doses of 0 to 9 Gy were used. It should be noted that experiments were performed in water environment (tubes with gel were located in water phantom. The DEF was calculated and result was as follow: The dose enhancement factors were 1.014±0.07, 1.074±0.11and 1.161±0.15 for 0.02, 0.05 and 0.1 mM concentrations, respectively [47].

From all these studies it is clear that polymer gel dosimetry plays an important role in metal NPs-aided radiotherapy and diagnostic, but this field still required additional investigations

In vivo studies were performed by M.Y Chang et al. (2008) to evaluate dose enhancement of gold nanoparticles [53]. B16F10 melanoma tumor-bearing mices were used in dose enhancement experiment [53]. The concentration of nanoparticles solution was 180μg/ml. The mices were injected with 200μl of this solution and the concentration of nanoparticles in organs was evaluated and resented in Fig. 10.Thes results helps to select the concentration of nanoparticles used in our investigation.

	Au (μg)/Tissue weight (mg)	
	PBS control	AuNPs
Tumor	1.79	74.24
Liver	0.26	147
Kidney	1.05	2.62
Lung	2.19	5.38
Spleen	2.86	350.55
Blood	0.71	1.46
Tumor surroundings	0.97	11.55

Fig.10. Accumulated nanoparticles concentration in different organs after injection [53].

1.6.1 Nanoparticles synthesis

Nanoparticles are particles between 1 and 100 nanometres size [1]. Plenty of methods are used for NPs synthesis these methods are basically categorized into two types: bottom-up and top-down methods [51]. Top-down is destructive method here, the bulk material reduces to nanoscale particles. Bottom up method based on atoms that aggregate into cluster and then form nanoparticles. The most suitable for this research nanoparticles synthesis method will be discussed below.

Chemical reduction is the most common method of metal (such as Ag) nanoparticles preparation. During this process the reduction agents are used for metal ions (from salt) reduction to metallic particles which agglomerate into oligomeric clusters. From these clusters are formed metallic colloidal nanoparticles. It is important to prevent aggregation of dispersive NPs during the course of metal nanoparticle preparation, for this reason the stabilizing agents are used that can be absorbed on or bind onto nanoparticle surfaces, avoiding their agglomeration [52]. In the case of Ag nanoparticles formation the reducing agents usually are odium citrate, ascorbate, sodium borohydride ($NaBH_4$), elemental hydrogen, polyol process, Tollens reagent, N, N-dimethylformamide (DMF), and poly (ethylene glycol)-block copolymers [52].

Photochemical method uses irradiation during nanoparticle synthesis. The variety of irradiation methods could be used: ultrasound, microwaves, UV light, laser. Silver nanoparticles were successfully synthesized using the UV irradiation of aqueous solutions containing $AgNO_3$ and gelatin by M. Darroudi et al. (2011) [53]. Using this method, aquatic solutions are exposed to UV-irradiation, during irradiation the hydrated electrons can be prodeced. These electrons reduce metallic cations to the metallic atoms and finally coalesce to form clusters [53]. The present of AgNP could be observed from solution color changes during irradiation, color gradually changed from colorless to yellow, then to brown, and finally dark brown [53].

Ionizing radiation such as are electron beam, X-ray, gamma-ray, could be also used for metallic nanoparticles formation [54]. Metal colloids are used in radiation-induced nanoparticles fabrication. Colloids are particles of metallic elements and their surrounding phase [54]. The metallic nanoparticles can be prepared in an aqueous solution in the presence of a stabilizer without using chemical reducing agents, namely by using of radiolytic method [54]. Then aqueous solution is irradiated the large number of hydrogen radicals and hydrated electrons are produced. These radicals are strong reducing agents; hence they can reduce metal ions into zero-valent metal particles [54]. With changes in radiation dose the number of produced metal particles can be controlled. Metal atoms which are produced during radiolytic process are dispersed homogeneously throughout the solution, because radiation can easily penetrate the bulk of the sample and randomly reduce metal ions. New formed zero-valent metal atoms act as individual center of nucleation and further coalesce with other new formed metal atoms. The metal clusters start to grow and form metal nanoparticles. The stabilizing agent are added in order to prevent agglomeration of nanoparticles, usually it is organic compounds (polyvinyl-pyrrolidone, polyvinyl alcohol, organic molecules containing ethanol and $C_{12}H_{25}NaSO_4$,) or metal oxides [56].

Gel dosimeters can be used as phantom and as dosimeter in one place. Huge benefit of the gel dosimeters is ability represent 3D dose distribution. MAGIC gel is in the interest of this research because of its fabrication simplicity (available in normoxic environment), excellent tissue equivalency, dose sensitivity and other factors. It is important to estimate nanoparticles impact on MAGIC dosimetric gel ability absorb ionizing radiation, because these data might be used in radiation therapy field. If nanoparticles enhancement dose in the gel volume, with same dose the higher energy absorption and higher damage could be achieved. Nanoparticles incorporation in gel introduces mechanism of radiation absorption in tumor with inserted nanoparticles. Nanoparticles incorporation in tumor volume could increase tumor damage from therapy procedures. Such dose distribution changes help to spare healthy tissue and protect organs at risk.

2. MATERIALS AND METHODS

2.1 GEL PREPARATION

The MAGIC gels were prepared based on recommendations presented by P. M. Fong at al. (2001) [29]. These chemical compounds were used in gels preparation:

- Gelatin from porcine skin (from Sigma - Aldrich, 99,995%)
- Methacrylic acid, contains 250ppm MEHQ as inhibitor (from Sigma-Aldrich, 99%)
- Hydroquinone (from Sigma-Aldrich, 99%)
- Copper(II)Sulphate Penthahydrate (from Lach-Ner, 93%)
- L-Ascorbic acid (From UAB Eurochemicals, 99,9%)
- Silver nitrate (from Sigma-Aldrich, 99,9%)
- Sodium citrate (from Sigma-Aldrich, 99%)
- Distilled water

11 polymeric gels were prepared for research, precise chemical composition of each gel given in Table 8.

Table 8. Chemical composition of 25g of each investigated gel.

Name	Gelatin, g	MAA, g	Hydroquinone,g	$CuSO_4*5H_2O$, g	Ascorbic Acid, g	$AgNO_3$ (1M), µl	Sodium Citrate, ml	H_2O, g
MAGIC(S)	2	2.25	0.05	0.0005	0.0088	-	-	20.7
Gelatin($AgNO_3$)	2,5	-	-	-	-	50	0.25, 5%	22.2
Gelatin(NPs)	2,5	-	-	-	-	50	0.25, 5%	22.2
MAGIC(9%)	2	2.25	0.05	0.0005	0.0088	-	-	20.7
MAGIC(6%)	2	1.5	0.05	0.0005	0.0088	-	-	21.45
MAGIC(3%)	2	0.75	0.05	0,0005	0.0088	-	-	22.2
MAGIC(NPs20mM)	2	2.25	0.05	0.0005	0.0088	500	0.2, 33%	20.7
MAGIC(NPs10mM)	2	2.25	0.05	0.0005	0.0088	250	0.2, 10%	20.7
MAGIC(NPs5mM)	2	1.75	0.05	0.0005	0.0088	125	0.25 10%	21.2
MAGIC(NPs2mM)	2	1.75	0.05	0.0005	0.0088	50	1, 1%	21.2
MAGIC (NPs1mM)	2	1.75	0.05	0.0005	0.0088	25	0.25, 5%	21.2

Gel preparation was performed in the fume hood. The gelatin was added to appropriate amount of distilled water (2 g gelatin and 17.5 g water in standard MAGIC) and left to swell for 10 minutes. The swelled gelatin was heated up to 50°C and stirred with a magnetic stirring until the gelatin fully dissolved (Fig. 11). The gelatin solution was cooled down 35-40°C and stirred. At temperature ~50 the 0.05 g hydroquinone in 1.2 g water was added. When gel has cooled ~37°, the appropriate amount of ascorbic acid (0.0088g in 1.25g water), $CuSO_4$ *$5H_2O$ (0.005g in 0.75g water) and MAA were added and stirred for more about 30min. In gels where MAA concentration was changed, the appropriate amount of water was added in firs step of gel preparation, compensating difference in MAA weight. The same procedure was repeated with each MAGIC gel. When gels preparation ended they were poured in to plastic cuvettes with diameter of 1cm and shut tight with plastic caps. After preparation gels were stored in cool dark closed until irradiation.

Fig.11. Gel preparation in fume hood.

2.2 SILVER NPS SYNTHESIS AND INCORPORATION IN GEL

Silver NPs were synthesized in photoreduction reaction using UV source. Two different methodologies were used for gels with silver NPs synthesized in photoreduction reaction.

In the first method MAGIC(NPs10mM) and MAGIC(NPs20mM) gels were prepared. The gelatin solution with already synthesized silver nanoparticles was used as gelatin basis for gel. This

solution was prepared by gelatin and water added $AgNO_3$ and sodium citrate and then, irradiated with UV lamp for 60min. This gelatin was then heated and stirring as basis for MAGIC gel formation and all required agents were added as described above.

In the second method MAGIC(NPs1mM), MAGIC(NPs2mM) and MAGIC(NPs5mM) gels were prepared as nanoparticles was synthesized after gel formation. During gel preparation after methacrylic acid is added and gel left for stirring in gels, where the nanoparticles should be produced, were added $AgNO_3$ as a precursor of nanoparticles and sodium citrate as stabilizing agent. After gel formation gels with added $AgNO_3$ were irradiated with UV lamp as shown in Fig. 12. The irradiation time was 60 minutes. The UV was reducing agent of nanoparticle synthesis. Synthesis proceeded by following reactions [53]:

$$\begin{gathered} H_2O \xrightarrow{UV} e_{aq}^- + H_3O^+ + H^\cdot + OH^\cdot + \ldots \\ Ag^+ + e_{aq}^- \xleftrightarrow{\text{Reduction}} Ag^o \\ H^\cdot + Ag^+ \xleftrightarrow{\text{Reduction}} Ag^\cdot + H^+ \\ Ag^o + Ag^+ \rightarrow Ag_2^+ \end{gathered} \tag{14}$$

During UV irradiation the radiolysis of water occurs and the solvated electrons are produced. These electros can reduce metallic silver cations to the atomic silver. Atomic silver and silver cations can interact and form charged nanosilver agglomerates [53]. The color of gel changes in present of nanoparticles from colorless to dark brown with respect of nanoparticles amount.

Fig. 12. Gels irradiation with UV source.

2.3 GEL IRRADIATION

The irradiation was performed in Lithuanian Health Sciences university's Kaunas Clinics filial – Oncology hospital. Varian Clinac DMX linear accelerator was used for the gel irradiation. 6 MeV beam energy was used and dose was from 0,5 Gy to 10 Gy. Irradiation was performed 2-7days after gel fabrication.

2.4 EVALUATION OF X-RAY IMPACT ON GEL

Three different methods were performed for the observation of radiation impact on gels physical properties.

The first method was examination using radiochromic films. The film was placed under the gel sample as shown in Fig. 15 during irradiation. The gel effect on absorbed dose changes in film were investigated in these measurements. After irradiation films was removed and scanned using scanner HP Scanjet G4050. Images were processed using *ImageJ* software and the normalized grey value related with optical density was calculated and evaluated with respect of radiation dose. The normalized optical density was calculated as average film gray level after irradiation ratio with 255 grey levels. Using *ImageJ* software average grey levels of film placed under the gel during irradiation was calculated. 255 gray levels exist where 255 means white and 0 means black, so the average distribution of grey levels (related to optical density), could be determined from average grey scale value and absolute value difference divided from absolute grey value.

Two types of radiochromic films were used:

- GafChromic RTQA^2. Dynamic dose range from 0,02 Gy to 8 Gy (Fig.13.). Self-developing film in real time, no additional processing required. High spatial resolution. Near tissue equivalency. Resistance at temperature up to 70°C [57].

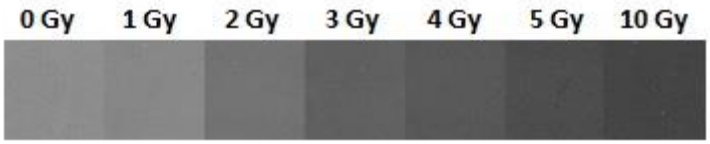

Fig.13. GafChromic RTQA^2 film irradiated with different ionizing radiation doses

- GafChromic EBT2. Dose range from 0,01 Gy to 10 Gy (measured in red color channel) up to 40 Gy (in green color channel) (Fig.14.). Yellow dye is incorporated into active layer which decreases UV/light sensitivity. Could be used to adjust small response differences in blue color channel. High spatial resolution. Near

tissue equivalency (100μm). Near tissue equivalent. Stable at temperature up to 60°C [58].

Fig.14. GafChromic EBT2 film irradiated with different ionizing radiation doses

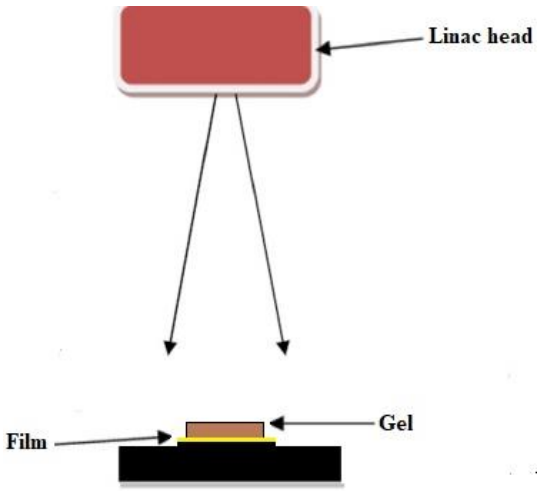

Fig.15. Scheme of gels measurements using film.

The second method was evaluation of X-ray transmission coefficient in gel using semiconductor detector "PTW CONNY II" presented in Fig. 16. The setup of the measurements is given in Fig. 17. "PTW CONNY II" is small size dosimeter used for quality assurance. Dosimeter measures the entrance dose and dose rate at 30kV/70kV/100kV [59]. Doses range from 20 nGy to 9,999 Gy. Nominal useful temperatures range from 10 to 40 °C.

In X-ray transmission evaluation experiments 200mGy dose was delivered to the samples and the dose under the cuvette was measured. Measurements were performed for the empty cuvette and gel filled cuvettes. X-ray transmission coefficient was calculated as a ratio between cuvette outgoing and incoming beams. Gulmay 3225 x-ray therapy unit was used for X-ray generation (120 KeV, 20mA and FSD 20cm).

Fig.16. Semiconductor dosimeter [59].

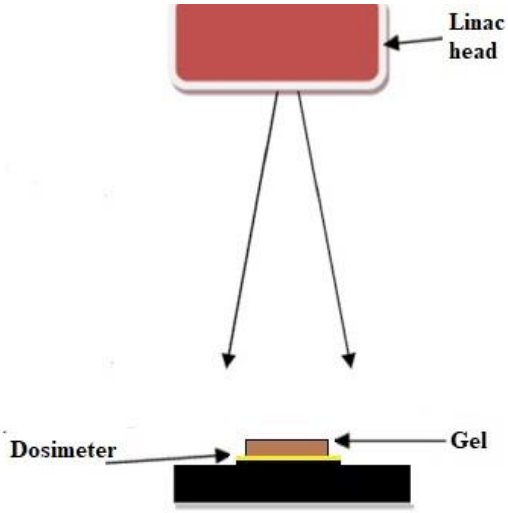

Fig.17. Transmission measurement using semiconductor detector.

After these measurements, the X-ray absorption coefficient, which define gel ability absorb radiation, was calculated using formula:

$$B=\left(1-\frac{D(x)}{D(0)}\right)\cdot 100\% \qquad (15)$$

where, D(x) – dose with sample, D(0) dose without sample.

Finally, USB4000 Fiber Optic Spectrometer was used for spectrometric measurements (Fig 18). Changes in optical gel properties were investigated using this technique. This spectrometer is responsive from 200-1100nm, but the specific range depends on parameters selected during setup [62]. Sensitivity of up to 130 photons/count at 400nm and 60 photons/count at 600nm. Integration times from 3,8ms to 10seconds [60].

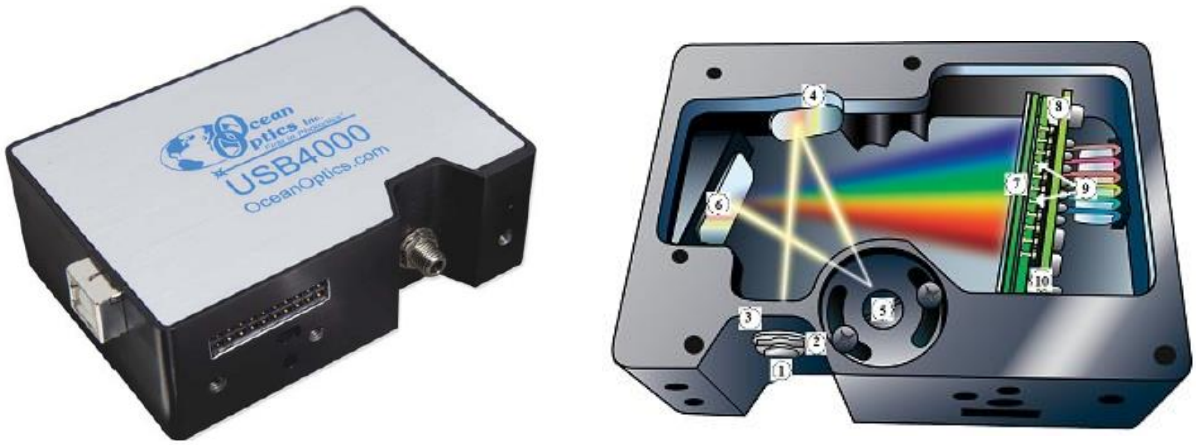

Fig.18. UV-VIS spectrometer USB4000. 1- Connector, 2- Slit, 3- Filter, 4- Collimating Mirror, 5- Grating, 6- Focusing Mirror, 7- Detector Collection Lens, 8- Detector, 9- Filters, 10 - Detector Upgrade [60]

The spectrometric measurements system consists of light source, optical fiber, spectrometer and "SpectraSuite" software. The measurement scheme is given in figure 19 [58]. The spectrometric system works as follow [61]:

- The light is released from the light source and transmits through an optical fiber to the cuvette with gel;
- Light interacts with the gel;
- Another optical fiber collects and transmits the result of the interaction to the spectrometer;
- The amount of light is measured by the spectrometer and the spectrometer transforms the collected data into digital information;
- The gel information is transferred from spectrometer to SpectraSuite;
- Software compares measurements from the gel to the reference measurements and display processed spectral information.

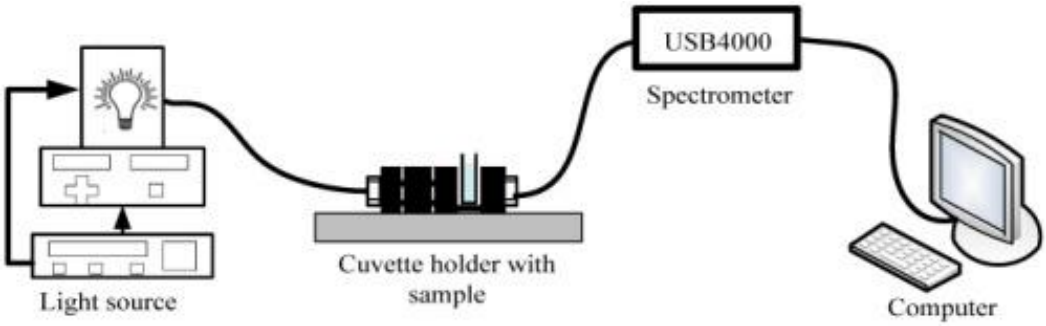

Fig.19. Scheme of spectrometric measurements [61].

Not all MAGIC gels spectra were measured because gels with higher silver nanoparticles concentration (from 2mM to 20mM) were not transparent to light.

The summary of applied investigation methods for each gel is given in table 9.

Table.9. Methods used to investigate gel physical properties after irradiation

Gel	Film dosimetry	UV-VIS	Attenuation measurements
MAGIC(S)	+	+	-
Gelatin($AgNO_3$)	+	+	-
Gelatin(NPs)	+	+	-
MAGIC(3%)	+	+	+
MAGIC(6%)	+	+	+
MAGIC(9%)	+	+	+
MAGIC(NPs20mM)	+	-	+/-
MAGIC(NPs10mM)	+	-	+/-
MAGIC(NPs5mM)	+	-	+
MAGIC(NPs2mM)	+	-	+
MAGIC (NPs1mM)	+	+	+

3. RESULTS AND DISCUSIONS

During this study 11 different chemical composition MAGIC gels were prepared and irradiated in order to evaluate X-ray absorption properties of the MAGIC gels and effect of ionizing radiation for gels physical properties. Equations and R^2 values of each trendline from graph are given in Appendix 1, Tables 1 and 2.

Firstly standard MAGIC gel was prepared according literature (P. M. Fong et al. 2001) – MAGIC(S) (See Table 8.). MAGIC(S) gel was irradiated using 6 MeV energy with 0.5 Gy, 1 Gy, 2 Gy, 3 Gy, 4 Gy and 5 Gy doses of X-ray irradiation. The gel samples before and after irradiation given in Fig. 20.

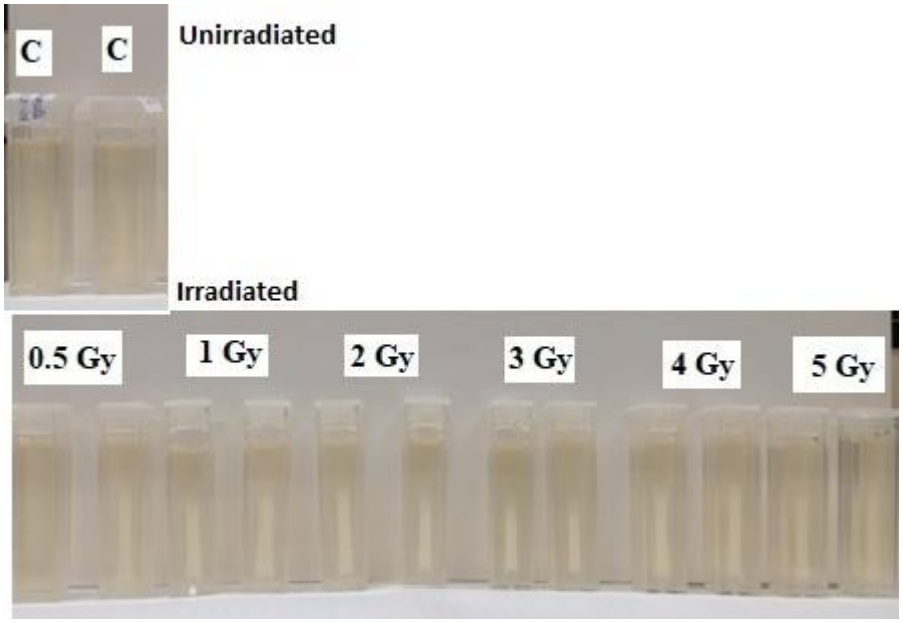

Fig.20. MAGIC(S) gel before and after irradiation.

After visual observation of the MAGIC(S) gel might be determined, that the radiation induced polymerization and crosslinking originates in irradiated gel. The white column in the middle of the cuvette it is a region of the polymerization. It is more concentrated were the radiation dose was higher.

Two types of GafChromic film were used for dose changes evaluation. The results are given in Fig. 21 and Fig. 22. Data shows that MAGIC(S) gel increases dose in gel compared with GafChromic film, which was irradiated without sample. However, the difference is not statistically significant. Such results might occur because the gel was in liquid form and copper ions could concentrate in the bottom of the cuvette. During copper ions interaction with radiation Compton scattering, backscattering might occur and photons from these reaction might reach the film inducing dose absorbed by film.

UV-VIS examination was performed before and after irradiation. The absorbance values at 550nm wavelength of irradiated gels are presented in Fig. 23. The results show that dose dynamic range of MAGIC(S) gel is from 0 Gy to 1Gy. In other regions dose was has no effect on light absorbance in gel. The results might be distorted, because of polymerization region presence in the middle of the cuvette, so UV-VIS method is unreliable at this point.

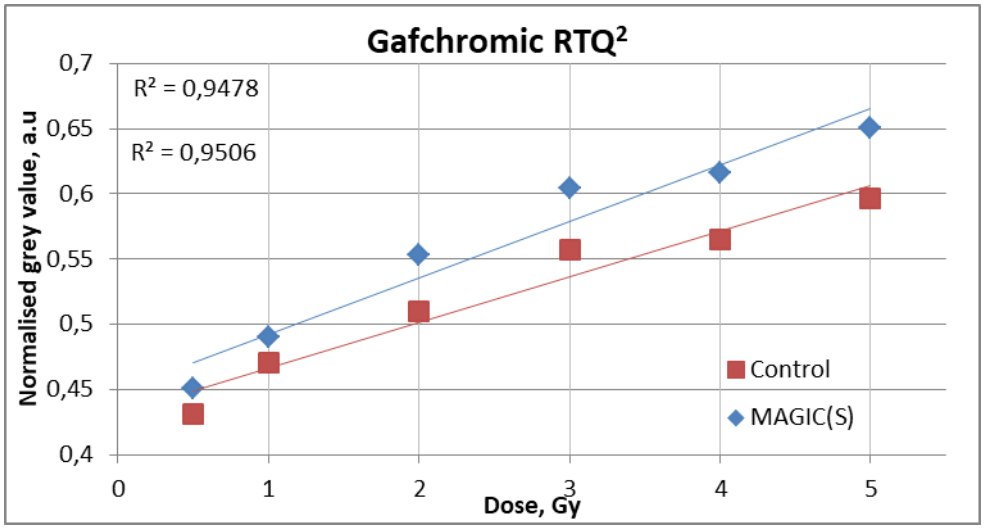

Fig.21. MAGIC(S) gel examination results using film

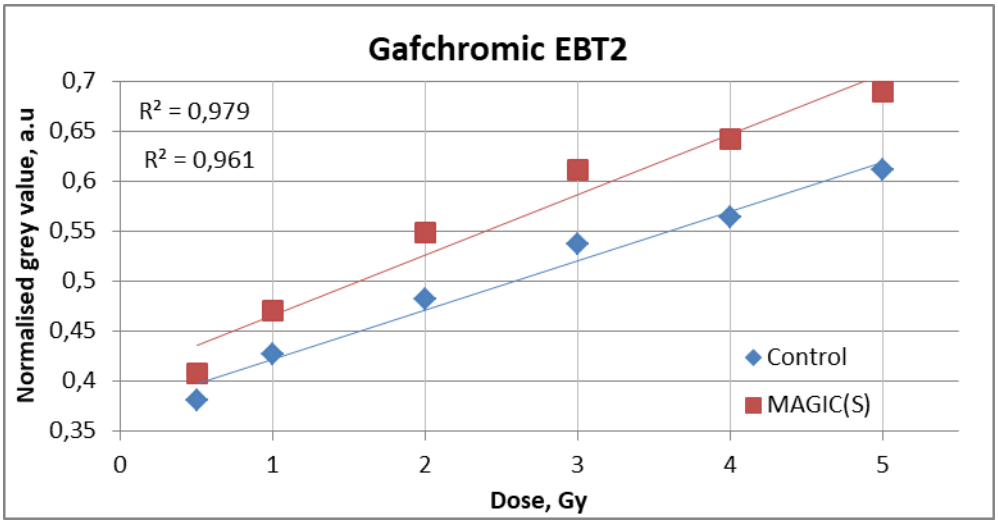

Fig.22. MAGIC(S) gel examination results using film.

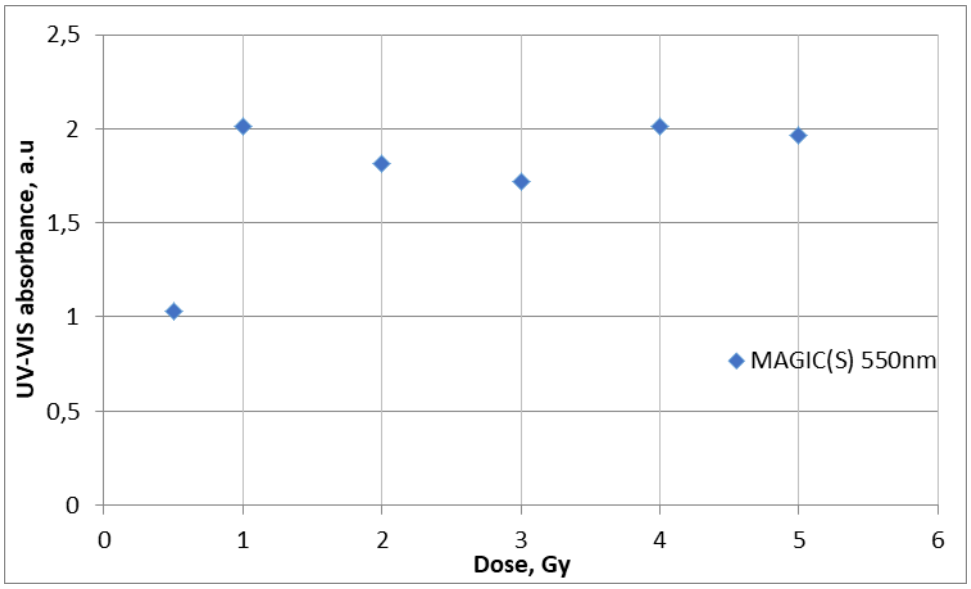

Fig.23. MAGIC(S) dosimetric gel response to irradiation dose at 550nm.

After this experiment, was decided investigate the ability of silver nanoparticles formation in gelatin under UV irradiation. Effect of silver salt ($AgNO_3$) and silver NPs incorporation in gelatin upon irradiation were tested as well. Two different gel were prepared for this purpose Gelatin($AgNO_3$) and Gelatin(NPs1mM) (see Table.8.). Gels were irradiated using 6 MeV energy with 1 Gy, 2 Gy, 3 Gy, 4 Gy and 5 Gy X-ray irradiation doses. Gels not change their visual appearance it could be seen from Fig.24 - 25, were Control (C) sample present un-irradiated gel.

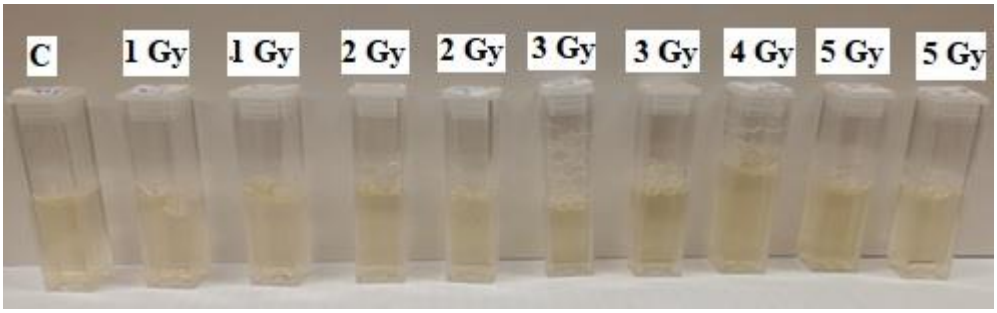

Fig.24. Gelatin($AgNO_3$) gels after irradiation.

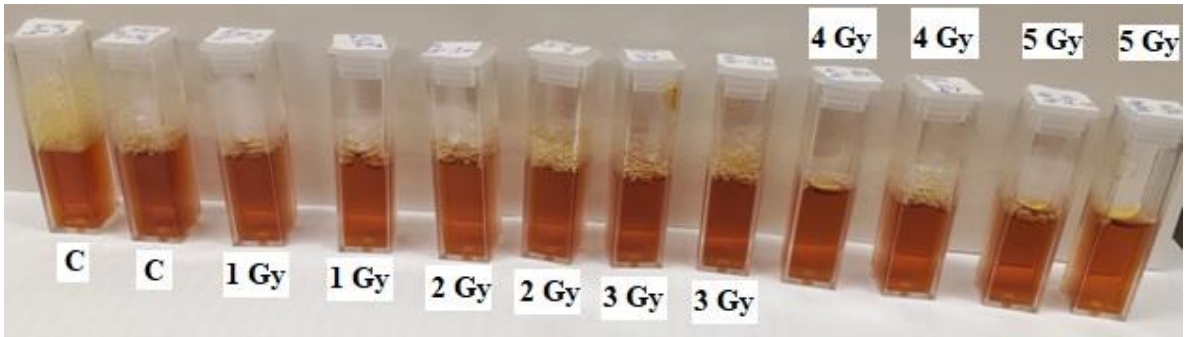

Fig.25. Gelatin(NPs1mM) gels after irradiation

The effect on X-ray dose, after passing the gel, was investigated using radiographic films. Results are presented in Fig 26, Fig. 27. The absorbed dose increment in film comparing control films and films under gel samples were detected.

The UV-VIS was applied in order to verify nanoparticles presence in Gelatin(NPs1mM) gel. The results are presented in Fig 28. From UV-VIS spectra it might be seen that peak appears in Gelatin(NPs1mM) at 400 -450 nm wavelength region, and in Gelatin($AgNO_3$) no peak is detected at this wavelength region. UV-VIS investigation proves presence of silver nanoparticles in Gelatin(NPs1mM) gel). It should be noted that no changes in Gelatin($AgNO_3$) and Gelatin(NPs1mM) gels UV-VIS spectra were detected comparing samples before and after irradiation.

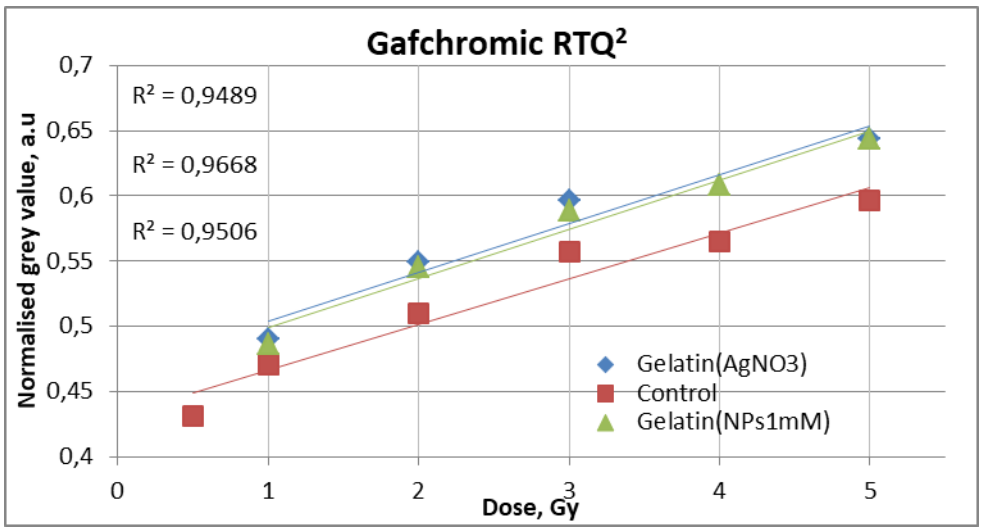

Fig.26. Gelatin($AgNO_3$) and Gelatin(NPs1mM) examination using film

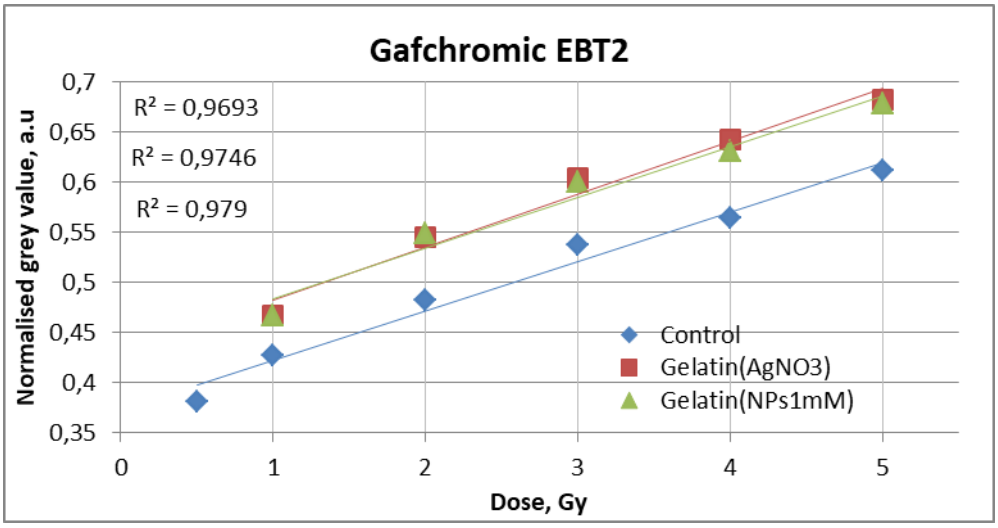

Fig.27. Gelatin($AgNO_3$) and Gelatin(NPs1mM) gels examination using film

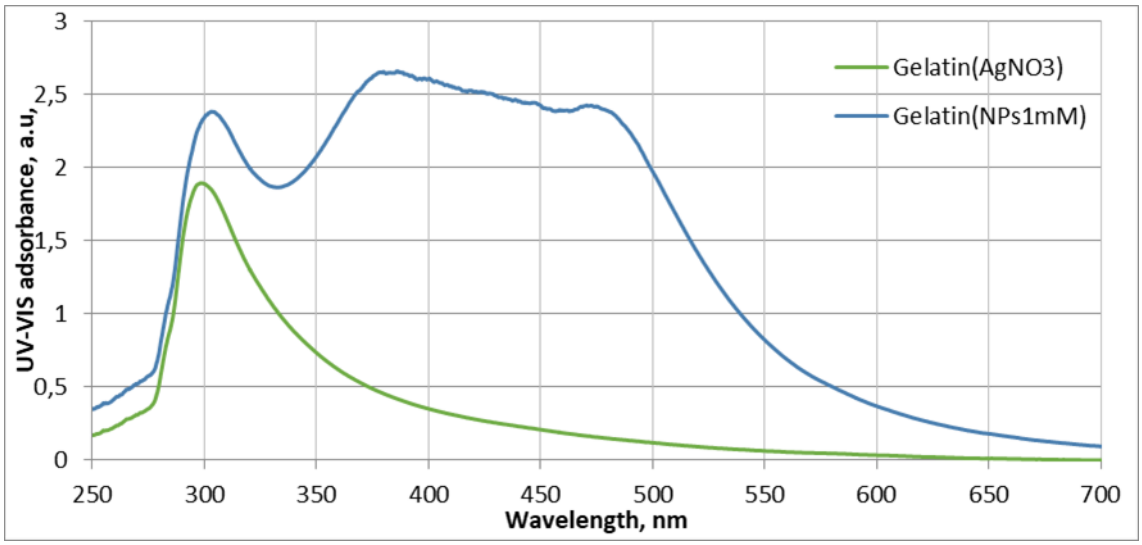

Fig.28. Comparison between Gelatin(AgNO3) and Gelatin(NPs1mM) gels UV-VIS spectrum

Effects of methacrylic acid concentration on gel qualities were investigated before nanoparticles incorporation in the gel. MAGIC gels with three different methacrylic acid concentration were prepared: MAGIC(3%), MAGIC(6%) and MAGIC(9%) (see Table.8.). These gels were irradiated with 1 Gy, 2 Gy, 5 Gy and 10 Gy X-ray irradiation doses. No visual changes were detected before and after irradiation of these gels, as it shown in Fig. 29, Fig.30 and Fig31, control gel sample (C) represents un-irradiated gel. However, it is apparent difference between colours of the gels (Fig 29-31). Gel with higher methacrylic acid concentration seems darker.

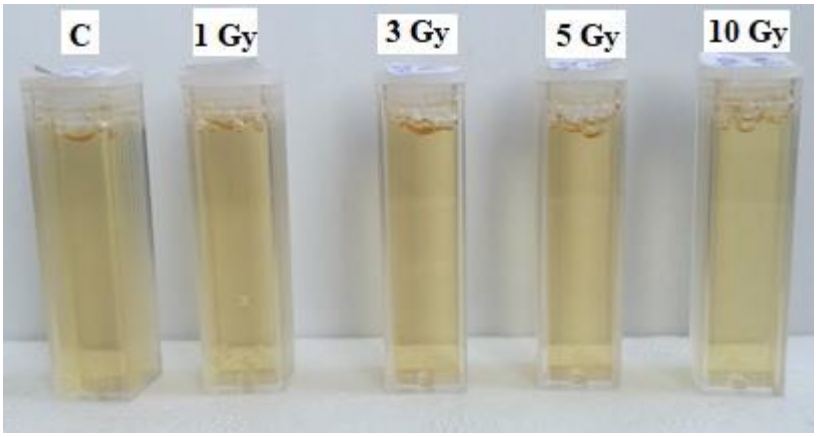

Fig.29. MAGIC(3%) gel after irradiation.

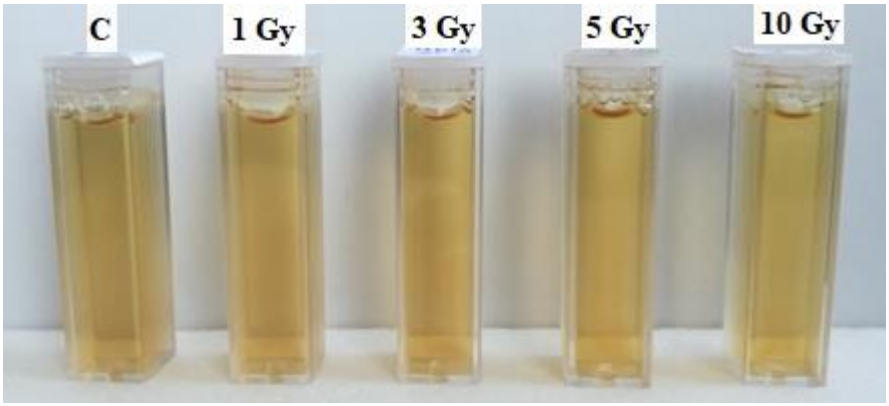

Fig.30. MAGIC(6%) gel after irradiation.

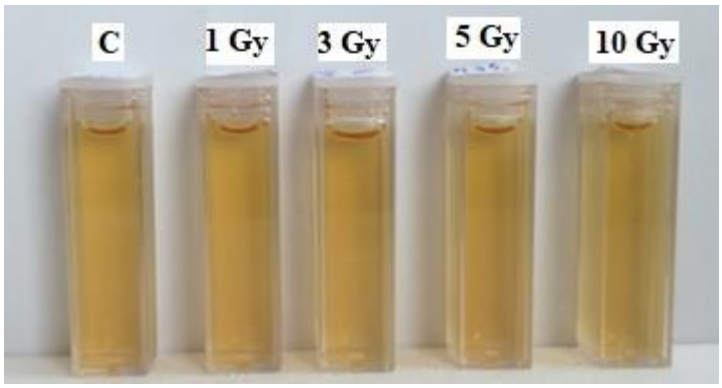

Fig.31. MAGIC(9%) gel after irradiation.

These three gels were investigated using GafChromicRTQ^2 film. The results of each gels is presented in Fig.32-34. The linear relation between dose and normalized grey value is notable for each gel. However, in comparison with control film no significant difference occurred.

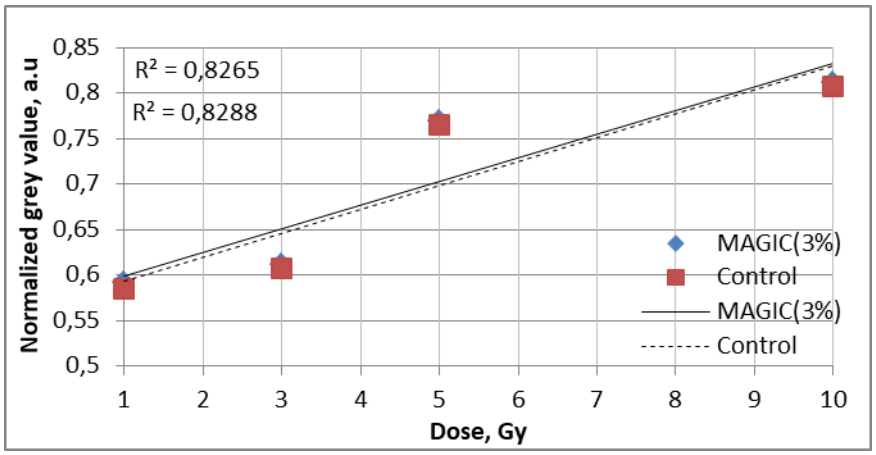

Fig.32. MAGIC(3%) gel measurements using film.

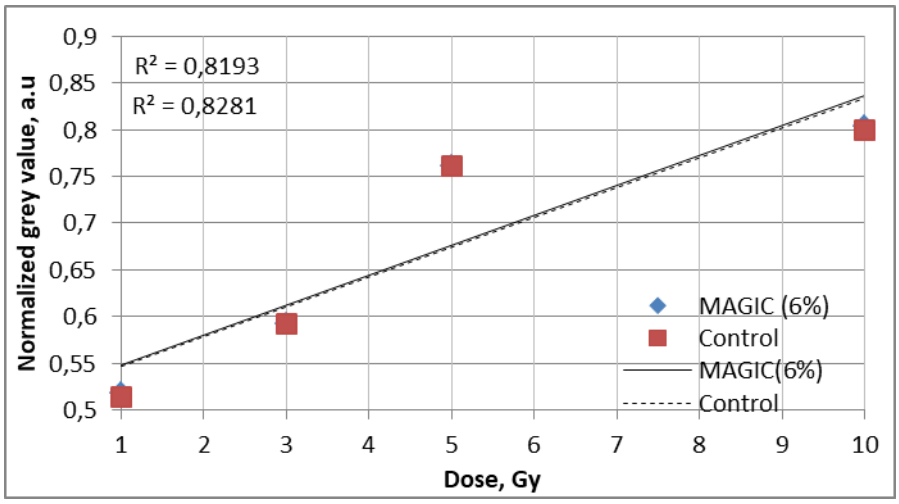

Fig.33. MAGIC(6%) gel measurements using film.

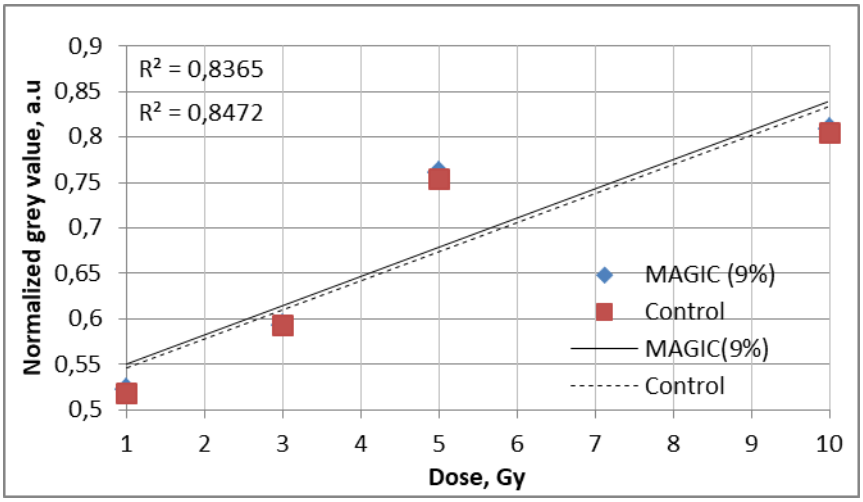

Fig.34. MAGIC(9%) gel measurements using film.

Comparison between MAGIC(3%), MAGIC(6%) and MAGIC(9%) was performed using results from measurement with film (Fig.35.). Results show that in dose range from 1 Gy to ~7 Gy, MAGIC(3%) dose absorbed in the film was highest, in the higher doses region no significant difference between these gels not observed. However, MAGIC(6%) and MAGIC(9%) shows better X-ray absorption properties, because dose absorbed in films which were placed under these gels was lower than with MAGIC(3%).

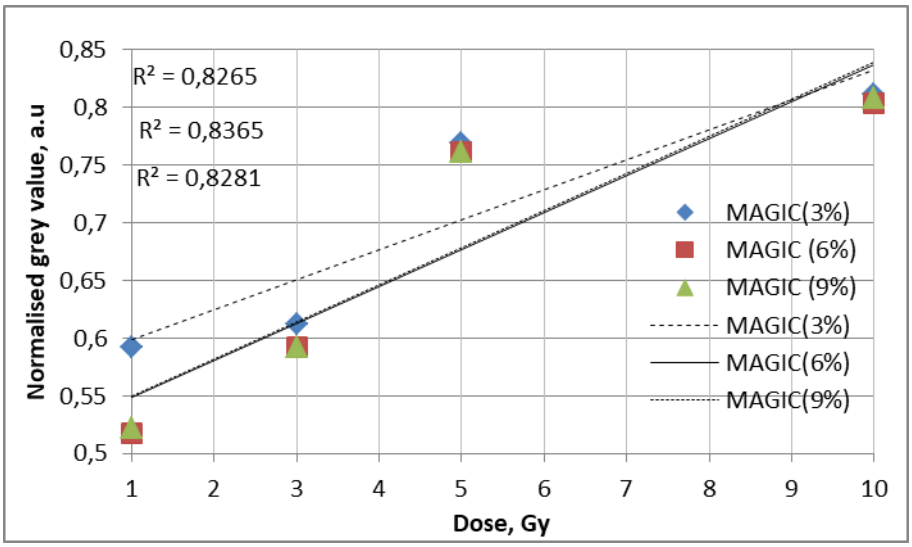

Fig.35. Dose sensitivity curves for MAGIC(3%), MAGIC(6%) and MAGIC(9%) gels evaluated using GafChromic films.

During this experiment was established that the optimal methacrylic acid concentration of the gel is between 6% and 9 %. MAGIC with 9% methacrylic acid liquefied and gel with 6% homogeneous gel consistence. Gel with 3% methacrylic acid concentration has lower dose reduction compared with 6% and 9% gels. With reference to these results was decided use 7% methacrylic acid concentration in successive gels.

After investigation using radiochromic film was made the X-ray absorption in gels were estimated by calculating absorption coefficient. The semiconductor detector was used for this purpose. Measurements were performed as described in figure 18. Radiation transmission was measured using detector and then X-ray absorption coefficient in gel was calculated according (15) formula. Measurements were performed before and after irradiation of gels. The results X-ray absorption coefficient values in gels with 6% methacrylic acid concentration before and after irradiation are given in Fig. 36.

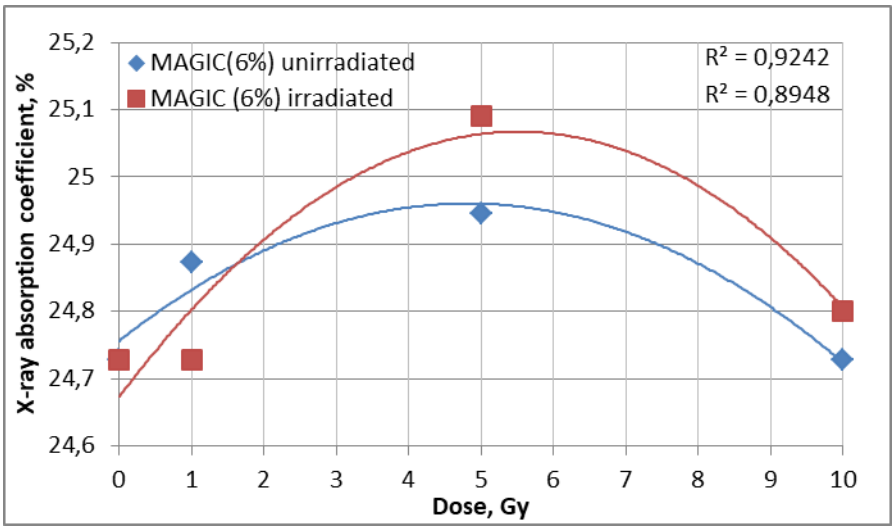

Fig.36. X-ray absorption coefficient values of MAGIC(6%) gel.

From these measurements it could be seen that in dose range from 1 Gy to 3 Gy the irradiation of the gel has no influence on X-ray absorption of gel, because the unirradiated gel has higher or same X-ray absorption sensitivity as irradiated in these dose range. The same tendency observed in all three gels. No one of gels had linear relation between irradiation dose and X-ray absorption coefficient. The dose measurements error of detector is ±2 %, such relation might occur because of this error. However, MAGIC(6%) irradiated gels have rise in absorption from 1 Gy to 5 Gy doses. The highest X-ray absorption coefficient was observed at 5Gy dose, such tendency could be observed in all three gels, but the strongest relation is in MAGIC(6%) irradiated gel samples. Absorption coefficients of irradiated MAGIC(6%) gel were 24.7%, 25.1%, 24.8% respectively 1 Gy, 5 Gy and 10 Gy irradiation dose. In the point of 5 Gy dose the absorption is increased and irradiated gel has higher absorption than unirradiated gel. Such relation might occur because of gel sensitivity for this dose range. So the optimal dose range in which MAGIC gels are useful in X-ray absorption is from ~0.5 Gy to 5 Gy.

Spectrometer was used in order to measure light absorption in irradiated MAGIC(3%), MAGIC(6%) and MAGIC(9%) gels. The results are given in Fig. 37. Measurements showed that absorption in gel is proportional to methacrylic acid concentration. The higher absorption was in MAGIC(9%), then in MAGIC(6%) and the lower absorption was remarked in MAGIC(3%) gel. Such conclusion also could be made by visual examination of these gels (Fig 29-31): gels with higher metharyclic acid concentration seems to be darker.

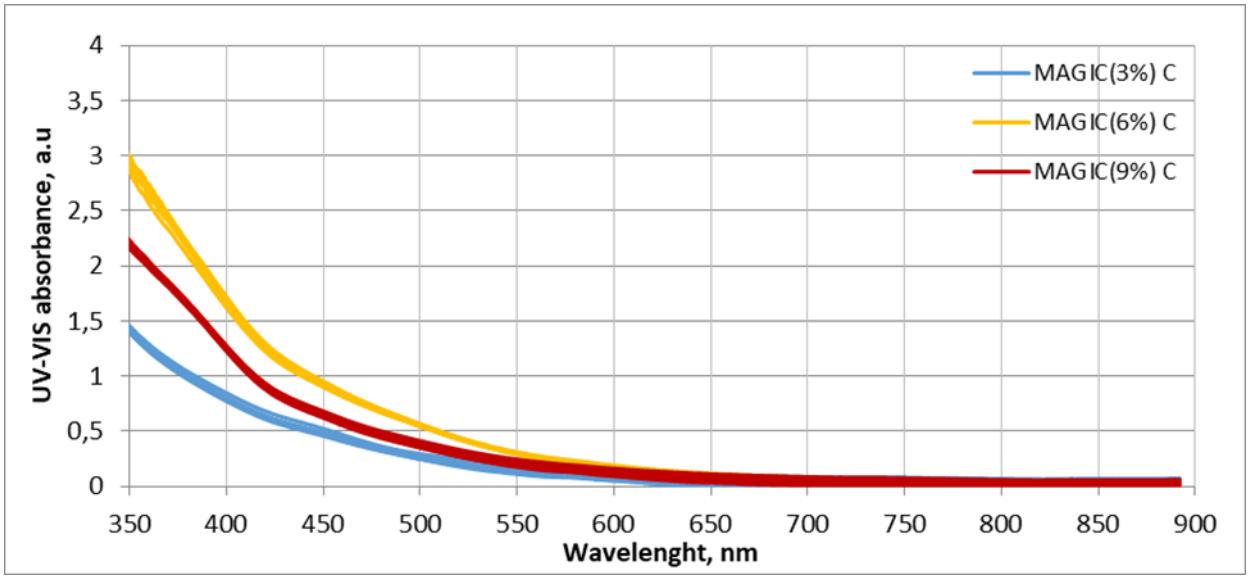

Fig.37. Spectrometric measurements of MAGIC(3%), MAGIC(9%) and MAGIC(6%) gels

2 Gy is mostly applied dose in radiation therapy. X-ray absorption in MAGIC(3%), MAGIC(6%) and MAGIC(9%) gels after 2 Gy irradiation was compared in order to evaluate optimal methacrylic acid concentration in this dose point. The results are given in Fig. 38.

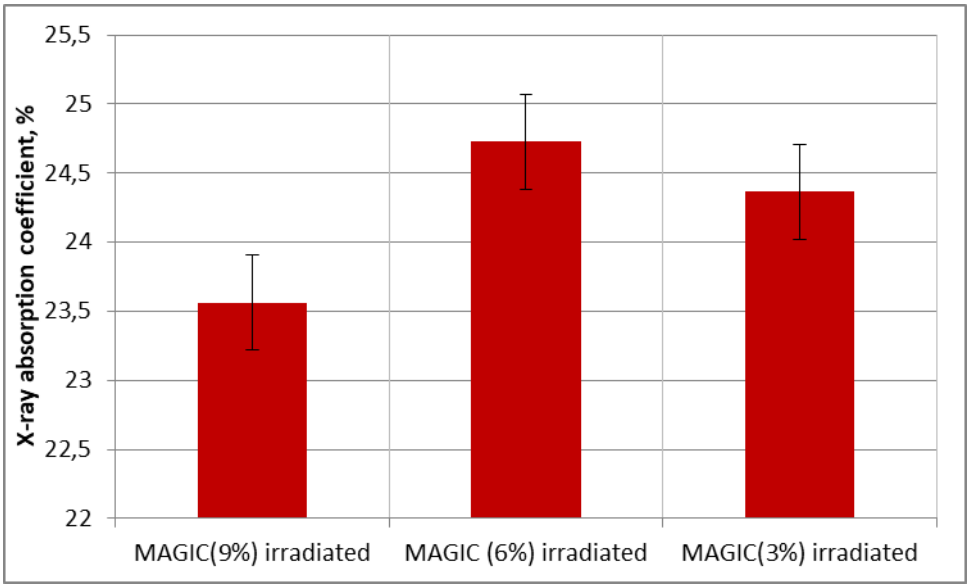

Fig.38. Comparison of X-ray absorption coefficient values in gels with different methacrylic acid concentrations. Measurements were performed at 2 Gy level.

The graph shows that the best X-ray absorption was in gel which had 6% concentration of methacrylic acid. The lowest absorption at 2 Gy dose point appeared in gel with 9% methacrylic acid concentration. The X-ray absorption coefficient in MAGIC(6%) gel was 24.7%, in MAGIC(3%) 24.4% and in MAGIC(9%) 23.5%. After statistical analysis was found out, that these

results was statistical significant with 95% reliability ($p<0.05$). The optimal methacrylic acid concentration at 2 Gy dose point indicated during research is 6% by weight.

Experiments with silver nanoparticles incorporation in gel begin with gelatin, where was added $AgNO_3$ as precursor for silver nanoparticles and sodium citrate as stabilizer. Silver nanoparticles in this solution were synthesis by UV irradiation. This gelatin solution was used as basis for MAGIC gel preparation. In this experiment two gels: MAGIC(NPs10mM) and MAGIC(NPs20mM) (see table 8.) were prepared and irradiated with 1 Gy, 2 Gy, 3 Gy, 4 Gy and 5 Gy doses of X-ray irradiation. How gels look after irradiation presented in Fig. 39 and Fig. 40. No changes in visual appearance were noticed before and after gel irradiation.

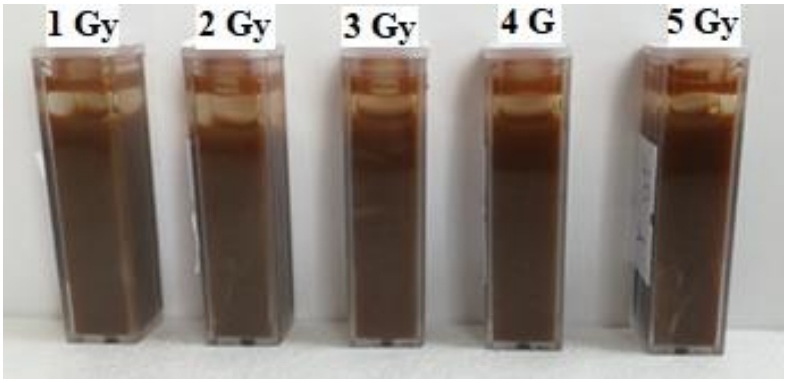

Fig.39. MAGIC(NPs10mM) gel after irradiation.

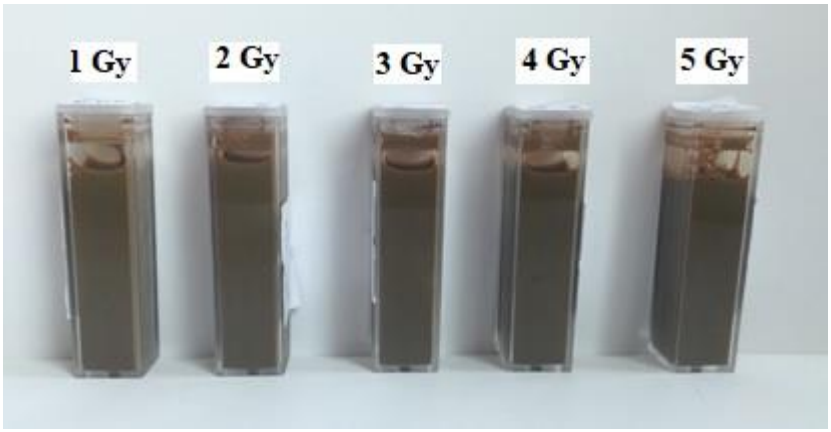

Fig.40. MAGIC(NPs20mM) gel after irradiation.

The results with radiochromic film are presented in Fig. 41. The dose enhancement on film compared with control is observed in MAGIC(NPs10mM) and MAGIC(NPs20mM) gels. Such results might be from additional photon interactions with silver nanoparticles in the bulk of gel, because the gel was liquid and silver nanoparticles were not homogeneous distribution, the photons from these reactions might reach the film and increase absorbed dose in the film.

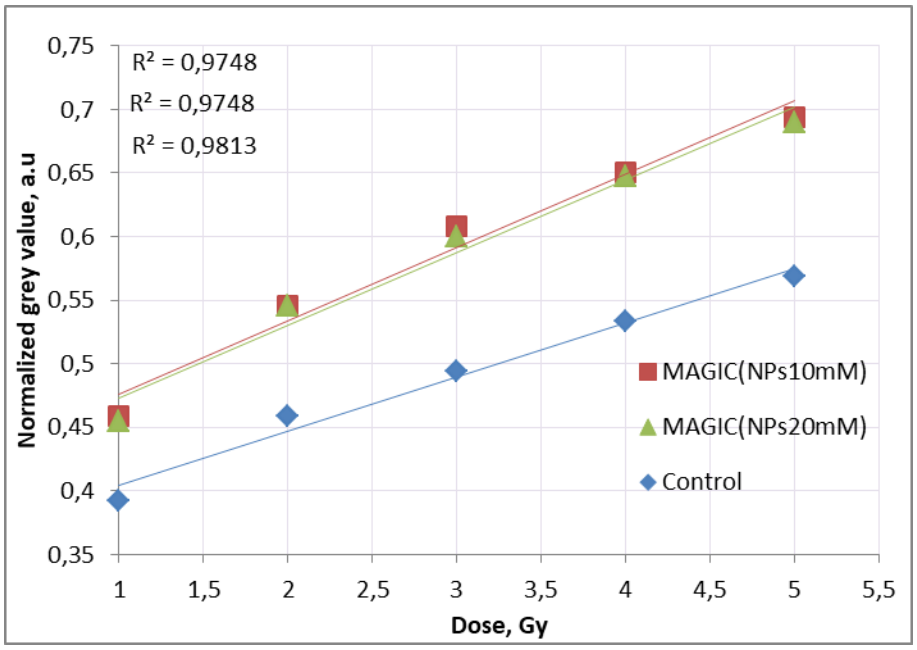

Fig.41. Comparison between MAGIC(NPs10mM) and MAGIC(NPs20mM) gel measurements using film.

Additionally X-ray absorption properties of these gels were evaluated using semiconductor detector. Measurement was accomplished using 120keV energy and nominal dose of 200 mGy. Firstly radiation dose was measurement without sample, then through cuvette, and eventually through gels, which was irradiated with 2 Gy radiation dose. The results are given in Fig.42.

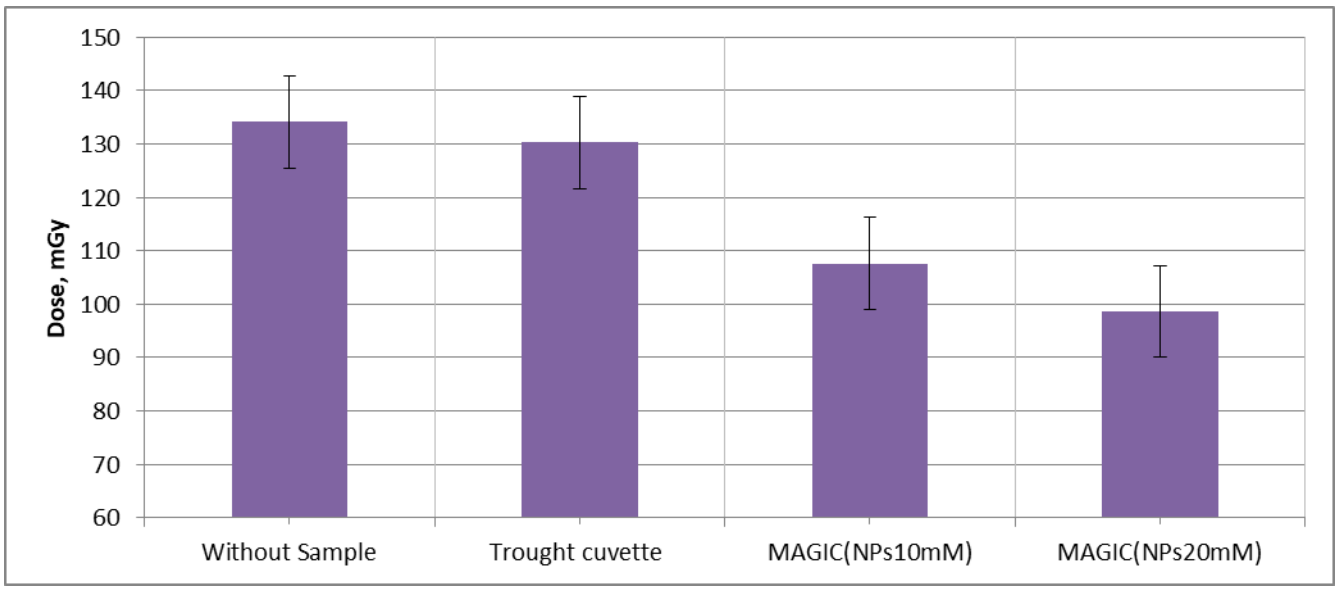

Fig.42. X-ray transmission in MAGIC(NPs10mM) and MAGIC(NPS20mM) gels irradiated with 2 Gy dose, measured using semiconductor detector.

The X-ray absorption coefficient was calculated in MAGIC(NPs10mM) and MAGIC(NPs20mM). The X-ray absorption coefficient value in MAGIC(NPs10mM) was 19.8%

and in MAGIC(NPs20mM) – 26.4%. This difference is statistically significant ($p<0.05$), this results confirmed that higher silver nanoparticles concentration improves X-ray absorption in gel.

UV-VIS measurements were not applied for these gels because they were opaque.

Next experiment was performed in order to evaluate if silver nanoparticle synthesis is possible in the already prepared MAGIC gel. 7% of methacrylic acid concentration was used based on previous investigation and gel formation issues. Firstly, gel MAGIC(NPs2mM) was prepared during procedure described in methodology (see Table 8.), in the end of gel preparation $AgNO_3$ and sodium citrate were added and then prepared gel was irradiated using UV lamp. After preparation the gel was homogeneous and color of the gel was light brown. The UV-VIS was obtained to evaluate silver nanoparticles presence in gel and the spectrum is presented in Fig.43. From the graph the small peak is perceived in 400-450nm wave length region, which proves silver nanoparticles presence in the gel.

However, in the progress of experiment the gel changes its appearance (fig.44.). The stratification occurred not only in irradiated gels but in control gel sample as well. The dark grey stratum formed in the bottom of gel. This might be the sediment of the silver. The gel consistency was sustained in MAGIC(NPs2mM), despite stratification of the gel.

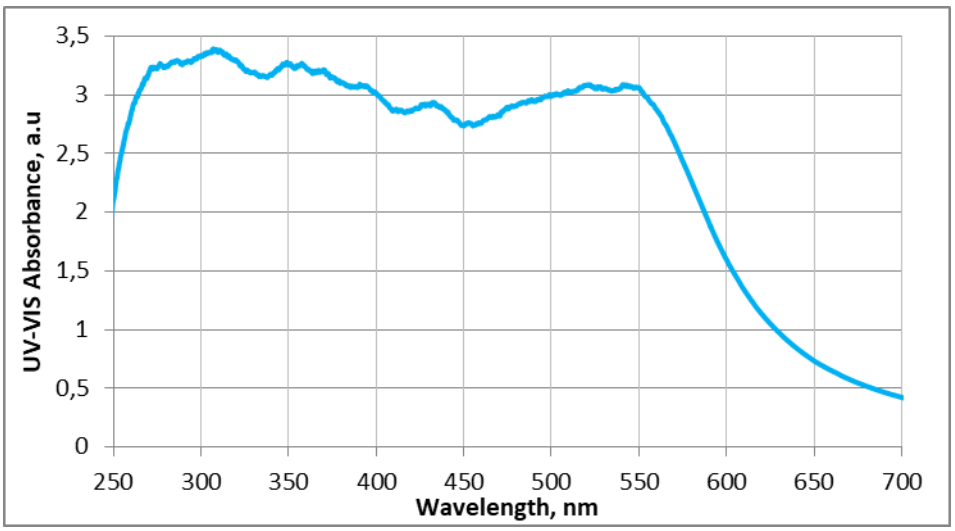

Fig.43. UV-VIS spectrum of MAGIC(NPs2mM) gel.

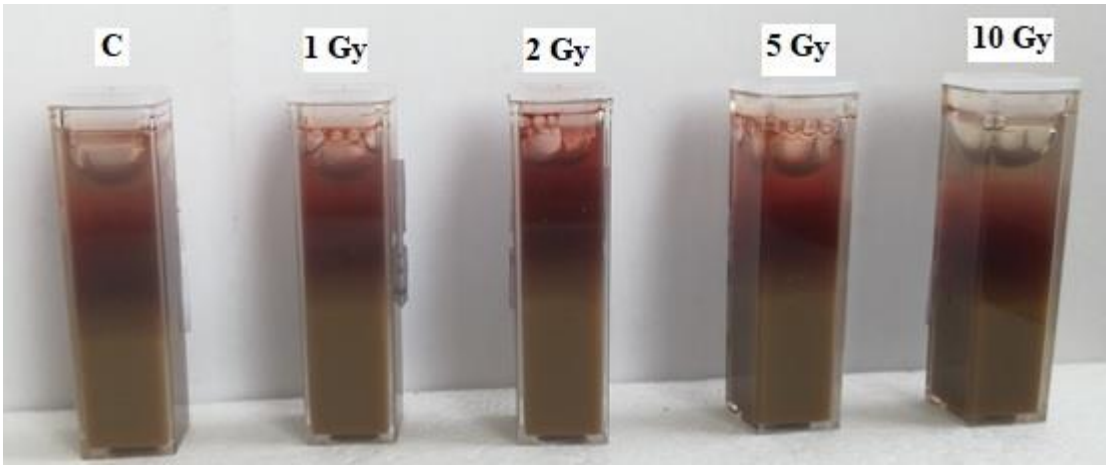

Fig.44. MAGIC(NPs2mM) gel after irradiation.

MAGIC(NPs2mM) gel was irradiated with 1 Gy, 2 Gy, 5 Gy and 10 Gy X-ray doses. No difference in film dose measurements between control film and film under MAGIC(NPs) were observed as presented in Fig 45.

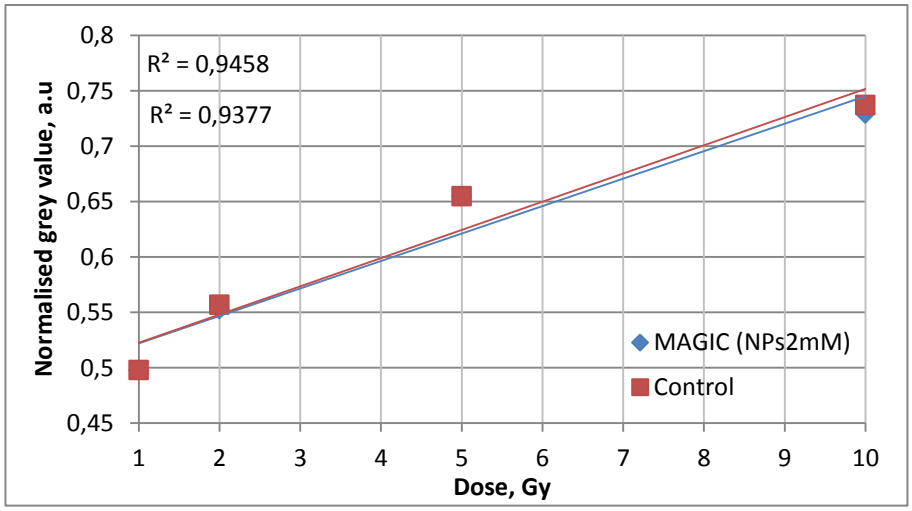

Fig.45. Results of MAGIC(NPs2mM) gel with film.

The ability to absorb radiation was also checked using semiconductor detector and attenuation coefficient calculation. Results of these calculations are presented in Fig. 46. The dependency of X-ray absorption coefficient value by the dose seems to be parabolic, such results might occur because of detector error (± 2%) [59]. In dose range from 1 Gy to 5 Gy absorption increases and then decreases. Results shows that with 5 Gy dose irradiated sample has the highest absorption coefficient – 26.7 %, while in other points absorption coefficient was 26.2 %, 26.4 %, 25.8 % respectively for 1 Gy, 2 Gy and 10 Gy irradiation doses. As is seen from the graph X-ray absorption of un-irradiated sample in the points of 2 Gy and 10 Gy irradiation doses are higher than irradiated sample.

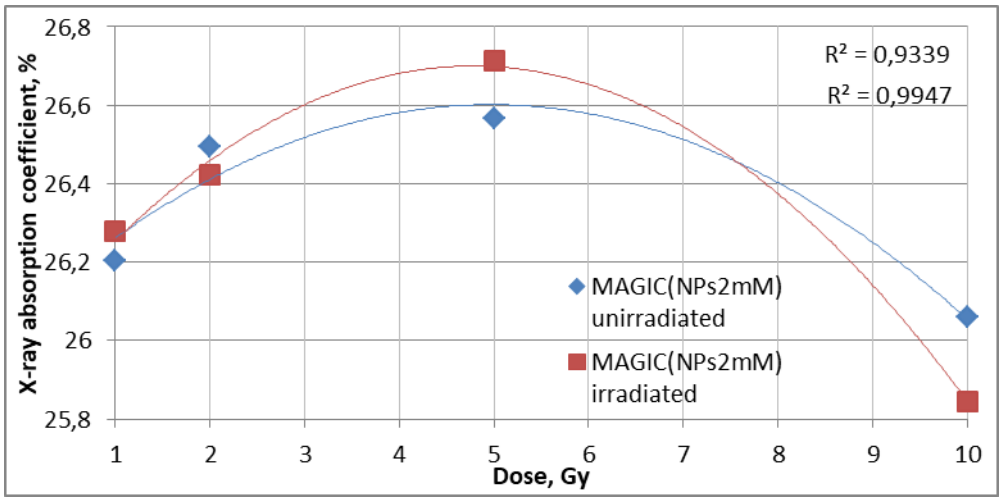

Fig.46. X-ray absorption coefficient values in MAGIC(NPs2mM) gel.

Additionally, two more gels with 1mM and 5mM nanoparticles concentration were prepared. In MAGIC(NPs1mM) and MAGIC(NPs5mM) (see Table.8.) gels silver nanoparticles were synthesized after gel formation as described in previous gel. Gels were pictured before and after irradiation and pictures are given in Fig 47 and Fig.48. Non irradiated gels were homogenous and have gel consistence. MAGIC(NPs5mM) gel were darker than MAGIC(1mM) gels, because of different silver nanoparticles concentration. Contrary gels after irradiation liquefied and lose their homogeneity. This might happened because of long period before gel preparation and irradiation.

MAGIC(NPs1mM) gel was measured using spectrophotometer in order to evaluate silver nanoparticles presence in the gel. With MAGIC(NPs5mM) gels such measurement was not performed because it was not transparent. The small peak might be determined at 450 nm wavelength, which proved silver nanoparticles presence in the gel.

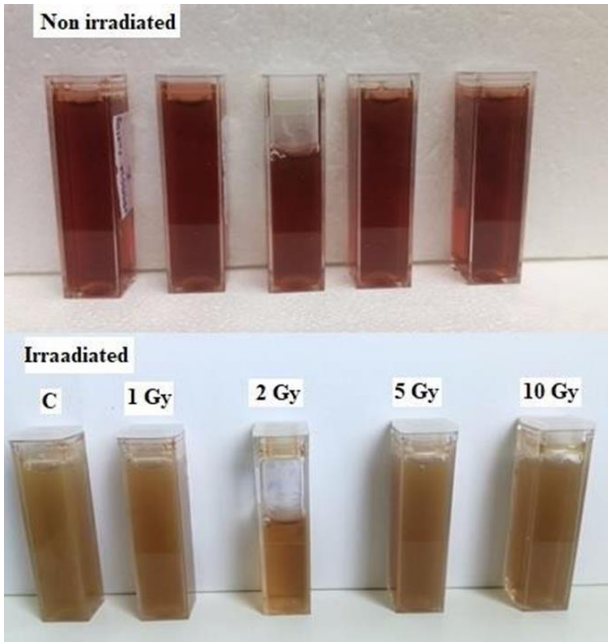

Fig.47. MAGIC(NPs1mM) gel before and after irradiation

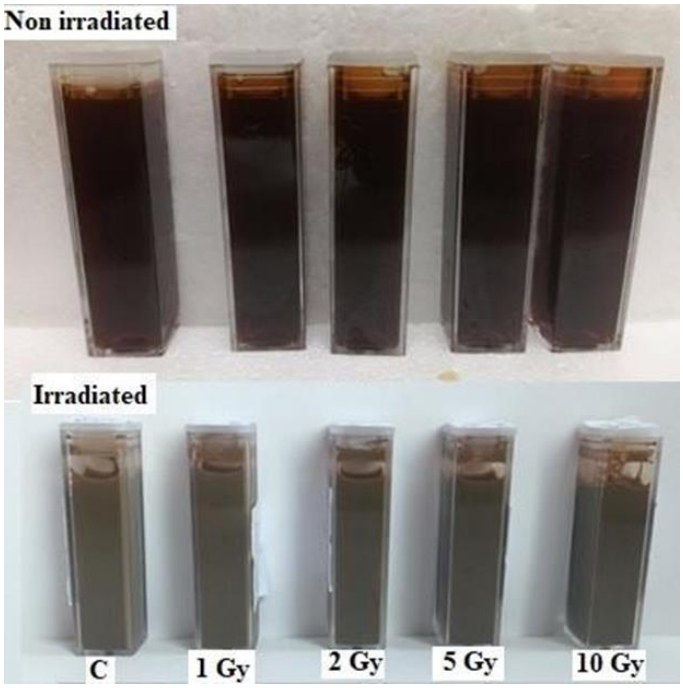

Fig.48. MAGIC(NPs5mM) gel before and after irradiation

In the last experiment MAGIC(NPs1mM) and MAGIC(NPs5mM) gels with different silver nanoparticles concentrations were irradiated with 1 Gy, 3 Gy, 5 Gy and 10 Gy X-ray doses. Firstly, the measurements using radiochromic film was made to absorbed dose evaluation, due to gel on radiochromic film. The results are given in Fig. 49 and Fig. 50. Comparison of MACIG(NPs1mM), MAGIC(NPs2mM) and MAGIC(NPs5mM) gels with different silver nanoparticles concentration measured using films given in Fig. 51. No significant effect on film dose was observed, the linear relation between dose and normalized grey value of the irradiated film was detected.

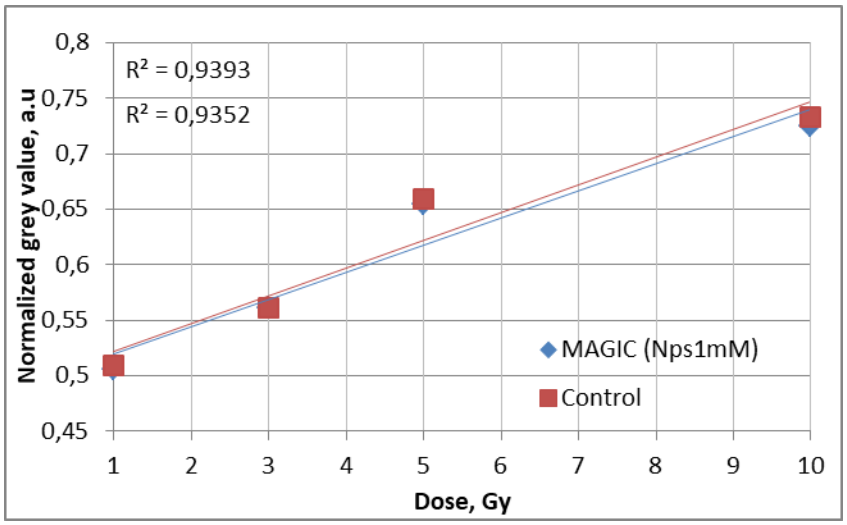

Fig.49. MAGIC(NPs1mM) dose measurements results with film

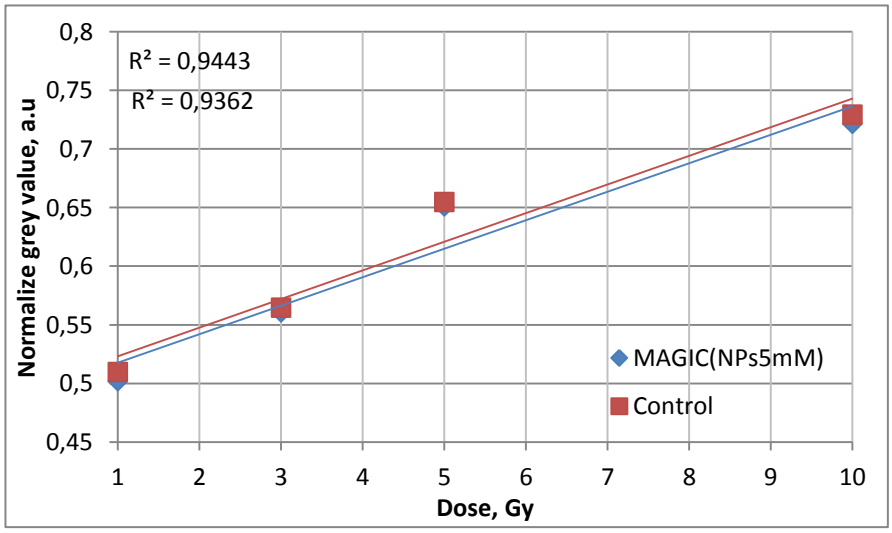

Fig.50. MAGIC(NPs5mM) dose measurements results with film

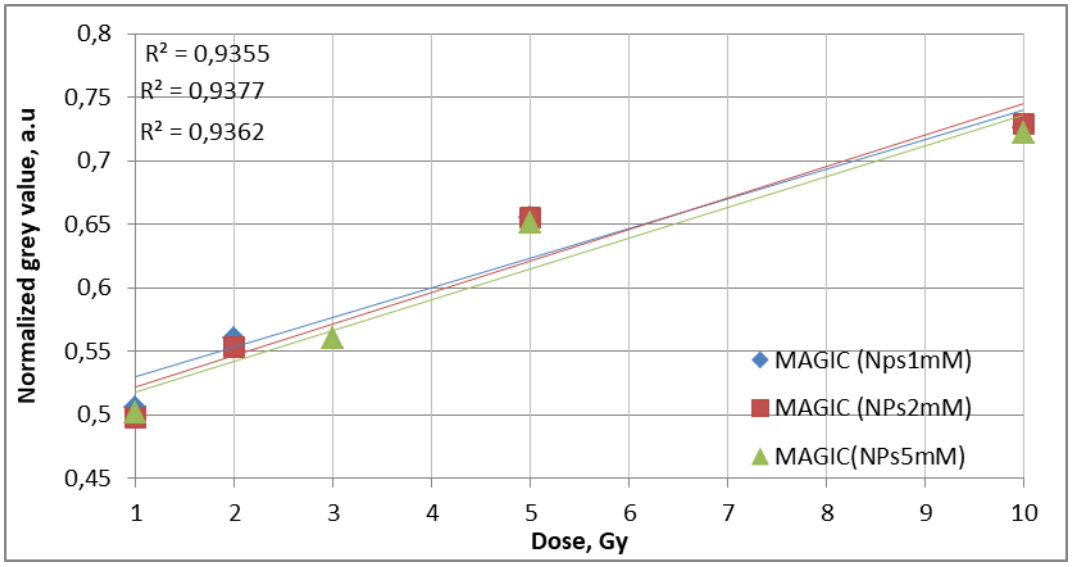

Fig.51. Comparison between MAGIC(NPs1mM), MAGIC(NPs2mM) and MAGIC(NPs5mM) gels properties using film.

Measurements with semiconductor detector of radiation attenuation in gel were made. From these measurements calculations were done. Results show that as distinct from gels with different methacrylic acid concentration (MAGIC(3%), MAGIC(6%), MAGIC(9%)) gels with varied silver nanoparticles concentration (MAGIC(NPs1mM), MAGIC(NPs2mM) ,MAGIC(NPs5mM) have increased X-ray absorption in 2 Gy dose point and decreased X-ray absorption in 5 Gy dose point. However, results present that un-irradiated gels has lower absorption coefficient values than irradiated gels. The highest absorption appears in MAGIC(NPs5mM) irradiated with 2 Gy, this gel absorb 23.9% of incident radiation. In MAGIC(NPs1mM) no relation between irradiation dose and X-ray absorption coefficient was determined. In MAGIC(NPs5mM) negative parabolic relation between gel radiation dose and X-ray absorption coefficient values was

observed. These results could be inaccurate because of long time period from gel preparation until irradiation (about 10 days).

Comparison between MAGIC (6%) and MAGIC(NPs2mM) gels was made in order to evaluate effect of silver nanoparticles incorporated in gel on radiation absorption properties of the gel. The calculations of X-ray absorption coefficients, after measurements with semiconductor detector, were applied for this purpose. The results are given in Fig. 52.

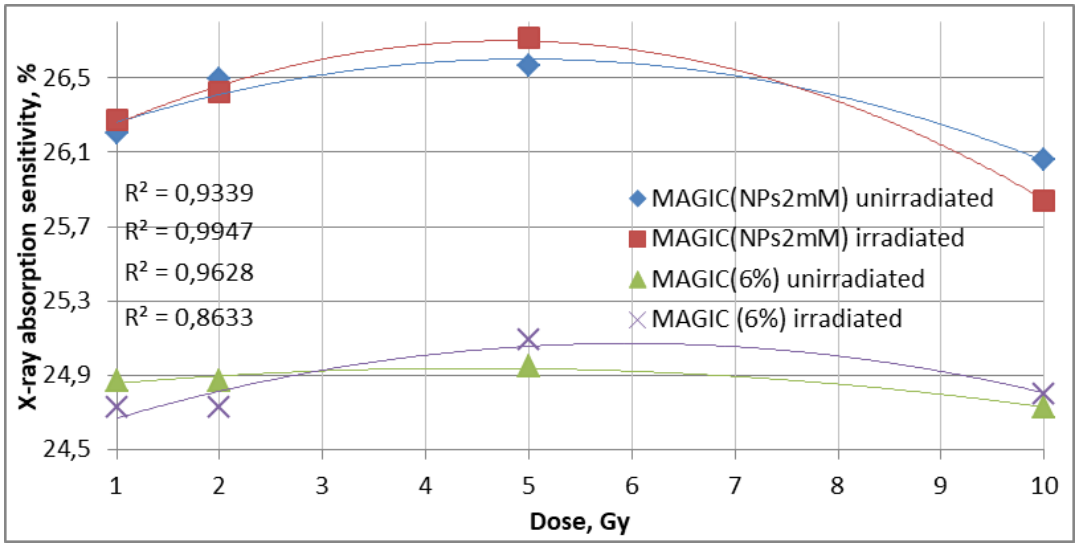

Fig.52. Comparison between X-ray absorption coefficient values in MAGIC(6%) and MAGIC(NPs2mM) gels.

These two gels was chosen because of similar methacrylic acid concentration: 6% in MAGIC(6%) and 7% in MAGIC(NPs2mM) and same irradiation doses: 1 Gy, 2 Gy, 5 Gy and 10 Gy. X-ray absorption coefficient values in irradiated MAGIC(6%) gel was from 24.7% to 25.1% and in irradiated MAGIC(NPs2mM) from 26.2% to- 26.7%. The highest X-ray absorption in both gels was at 5 Gy point. Statistical analysis show that MAGIC(NPs2mM) has higher absorption than MAGIC(6%) with 95% reliability ($p<0.05$). Difference at 5 Gy dose point was 1.6 %, at 1 Gy point – 1.6 %, at 2 Gy point – 1.7 % and at 10 Gy point – 1.0 % . From these result could be noticed that 2 mM silver nanoparticle concentration increases X-ray absorption by ~1.6 % compared with MAGIC gel without nanoparticles.

To sum up experimental results it reveal, that best absorption of ionizing radiation occurs in MAGIC(NPs2mM) gel and it was 26.6% at 5 Gy irradiation dose. The highest X-ray absorption coefficient at 2 Gy dose point was in MAGIC(NPs20mM) gel. The optimal methacrylic acid concentration was decided to be between 6% and 9% by weight because gel has stable and homogeneous structure using 6% and here was some problem with gel structure in 9 % gels.

Comparison between MAGIC with and without incorporated nanoparticles shows that silver nanoparticles could improve gel X-ray absorption properties.

The data also shows that ionizing radiation and time from gel preparation till irradiation have influence on gel physical properties, such as color and consistency. In standard MAGIC gel (MAGIC(S)), the polymerization region appears after irradiation. In gels with silver nanoparticles the color of gels changes and the gel liquefied in most cases.

From the equations of each gel trendline using film or/and semiconductor detector *a*, *b* and *c* coefficients were evaluated (Appendix 1). The summary of these coefficients is given in Table 9.

Table 9. Summary of trendline equations coefficients of gels.

Gel name	a (a^2) coefficient value		b coefficient value		c coefficient value
Results from film measurements					
MAGIC(S)	0.0433	0.0604	0.4489	0.406	
Control	0.0349	0.0494	0.4313	0.373	
Gelatin($AgNO_3$)	0.0373	0.0529	0.467	0.4294	
Control	0.0349	0.0494	0.4313	0.373	
Gelatin(NPs1mM)	0.0376	0.0506	0.4612	0.4333	
Control	0.0349	0.0349	0.4313	0.372	
MAGIC(3%)	0.026		0.527		
Control	0.0263		0.5662		
MAGIC(6%)	0.032		0.5165		
Control	0.0319		0.5151		
MAGIC(9%)	0.0322		0.5178		
Control	0.032		0.5147		
MAGIC(NPs20mM)	0.0573		0.4184		
Control	0.0427		0.3612		
MAGIC(NPs10mM)	0.0573		0.4157		
Control	0.0427		0.3612		
MAGIC(NPs2mM)	0.0248		0.4974		
Control	0.0255		0.4972		
MAGIC(NPs1mM)	0.0244		0.4956		
Control	0.0251		0.4966		
MAGIC(NPs5mM)	0.0244		0.4987		
Control	0.0243		0.4934		
Results from measurement using semiconductor detector					
MAGIC(6%) un-irradiated	0.0108		0.1248		24.645
MAGIC(6%) irradiated	0.0186		0.0829		24.5754
MAGIC(NPs2mM) un-irradiated	0.0216		0.2146		26.064
MAGIC(NPs2mM) irradiated	0.0313		0.299		25.986

The *a* coefficient present dose sensitivity (absorbance per grey), *b* coefficient present initial sensitivity (initial absorbance). The results show tendency, that dose sensitivity increases comparing measurements with and without gel using film. Same tendency occurs in measurement with semiconductor detector between irradiated and un-irradiated gels. Such results based on

radiation induced processes in the volume of gel. The cross-linking in MAGIC gels occurs upon irradiation and dose sensitivity increases because of increasing density of the gel. Gels with added silver nanoparticles also have higher dose sensitivity, because of photoelectric effect, Compton scattering and Auger electron formation during photon interaction with silver nanoparticles incorporated in gel. *C* coefficient is also initial coefficient defined equipment influence.

In comparison with this research results the optimal concentration of methacrylic acid in MAGIC gel was suggested as 9% by weight (P. M. Fong et al. 2001) [29]. But here was an additional investigation was the MAGIC chemical composition was investigated [55]. J. J. Luci et al. suggested that the optimal concentration is 4% because in this concentration the dose sensitivity is lower and lower dose sensitivity is useful for wider range of doses. [55]. According this author here is no significance effect of methacrylic acid concentration in gel higher than 4% for gel dosimetric properties.

Optimal gelatin concentration in gels is defined as 8% [55, 32]. In this research also 8% of gelatin was used and this concentration was appropriated for MAGIC gel radiation absorption examination.

Here was several investigation of dose enhancement in gels by adding nanoparticles, usually gold nanoparticles is used [45, 48-51]. M. Hassan et al. investigate dose enhancement using silver nanoparticles in MAGICA gel (Methacrylic Ascorbic in Gelatin Initiated by Copper with Agarose added) here was used 0.05 mM and 0.01 mM concentration of silver nanoparticles. Gels were irradiated with 5 Gy and 10 Gy dose, and magnetic resonance imaging for dose enhances evaluation was used. Results show that increasing nanoparticle concentration increases dose in gel [44].

H. Khosravi and colleagues made similar investigation of nanoparticles effect on dose enhancement in the external radiation therapy [47]. MAGICA gel was used with 0.02 mM, 0.05 mM and 0.1 mM. gold nanoparticles concentrations. The maximum 1% dose enhancement was determined compared gels with and without nanoparticles.

So the tendency that nanoparticles increases dose in gel consequently and X-ray absorption in gel was determined in this research. It should be noted that radiation absorption in gel measurements using film and spectrometric analysis could be less sensitive technique than magnetic resonance imaging so the results could be not such accurate and precise. However, nanoparticles incorporation in gel can improve X-ray absorption in gel and such gels could be used in clinical environment as tool for dose optimization and verification during radiation therapy treatments.

CONCLUSIONS

1. The theoretic overview was made in order to evaluate polymer gels used in medical applications, their advantages and disadvantages was presented and MAGIC gel was selected as most suitable for this research, because of its tissue equivalence, dose sensitivity, preparation and storage simplicity,
2. Eleven different chemical composition polymeric gels were prepared and the influence on X-ray absorption in gel was examined using GafChromic film and semiconductor detector measurements. For this purposed the metacrylic acid concentration and nanoparticles concentration were varied in gels. The optimal methacrylic acid concentration in 2 Gy region was 6%. MAGIC(NPs2mM) gel have best X-ray absorption and dosimetric qualities.
3. Silver nanoparticles were produced in gel by the photoreduction reaction. UV-VIS spectrometry was used in order to examine optical properties of gels and approve silver nanoparticles presence in gel. In one case silver particles were synthesized before gel formation and in other case in the process of the gel formation. The better qualities appears in gels were nanoparticles were synthesized after gel formation.
4. Investigation shows that MAGIC gels modified by silver nanoparticles improve X-ray absorption in gel. The results shows that best absorption qualities was in gel where methacrylic acid concentration was 7 % and nanoparticles concentration was 2 mM, X-ray absorption coefficient in this gel was 26.6 % at 5 Gy point.

REFERENCES

1. C. Baldock, Y De Deene, S. Doran, G. Ibbott, A. Jirasek, M. Lepage, K. B. McAuley, M. Oldham, L. J. Schreiner „Polymer gel dosimetry“, „*Physics in Medicine & Biology“*, 2010 February.
2. D. Titus, E. J. J. Samuel, S. M. Roopan, „Current scenario of biomedical aspect of metal-based nanoparticles on gel dosimetry“, *„Applied Microbiology and Biotechnology“*, 2016 April.
3. L. J. Schreiner, „Review of Fricke gel dosimeters“, „*Journal of Physics: Conference Series“*, 2004.
4. Institute of Medicine Committee for Review and Evaluation of the Medical Use Program of the Nuclear Regulatory Commission; Gottfried KLD, Penn G, editors. „*Radiation In Medicine: A Need For Regulatory Reform*“, Washington, National Academies Press (US); 1996.
5. R. Baskar, K.Ann Lee, R. Yeo, K. Yeoh, „Cancer and Radiation Therapy: Current Advances and Future Directions“, „*Global Cardiology Science and Practice*“, 2012 February.
6. G. Koukourakis, N. Kelekis, V. Armonis, V. Kouloulias, „Brachytherapy for Prostate Cancer: A Systematic Review“, *Advances in urology,* 2009 September.
7. E. J. Hall, D. J. Brenner, „Cancer risks from diagnostic radiology“, *The British Journal of Radiology*, 2008 February.
8. R. Sharma, S. D. Sharma, S. Pawar, A. Chaubey, S. Kantharia, D. A. R Babu, „Radiation dose to patients from X-ray radiographic examinations using computed radiography imaging system“. *Journal of Medical Physics / Association of Medical Physicists of India*, 2015 March.
9. The Royal College of Radiologist: Clinical Oncology „*Radiotheraphy dose fractionation. Second edition*“, 2016 December.
10. D. Fulea , C. Cosma , I. G. Pop, „Monte Carlo Method For Radiological X-Ray Examinations“, *Nuclear Medicine*, 2008 December.
11. S. Söderström, An. Eklöf, A. Brahme, „Aspects on the Optimal Photon Beam Energy for Radiation Therapy“, *Acta Oncologica,* 1999.
12. F. H. Attix „*Introduction to Radiological Physics and Radiation Dosimetry*“,Germany, 1968
13. *„Diagnostic Radiology Physics A Handbook for Teachers and Students“*, IAEA, Vienna, 2014.
14. http://bookpromos.lww.com/wp-content/uploads/2014/03/ch05_Interactions-of-Ionizing-Radiation.pdf
15. Mž. Donya, M. Radford, A. ElGuindy, D.Firmin, M. H. Yacoub , „Radiation in medicine: Origins, risks and aspirations“, *Global Cardiology Science and Practice*, 2014 December.
16. B. H.Tonnessen, L. Pounds, „Radiation physics“, *Journal of Vascular Surgery*, 2011 January
17. E. B. Podgoršak „*Radiation Physics for Medical Physicists. Third edition*“, Springer, 2016

18. Lithuania Hygiene Standard HN 73:2001 “Basic Standard of Radiation Protection”.
19. J. Seco, B. Clasie, M. Partridge, „Review on the characteristics of radiation detectors for dosimetry and imaging“, *Physics in Medicine & Biology*, 2014.
20. W. R. Hendee, E. R. Ritenour, „*Medical Imaging Physics. Fourth edition“*, Wiley-Liss, Inc., New Yor, 2002
21. http://www-naweb.iaea.org/nahu/DMRP/documents/Chapter3.pdf
22. D.Adlienė, R. Adlytė „Dosimetry Principles dose mesurements and radiation protection“, *Application of ionizing radiation in materials processing*, 2017, Vol.1, Warsawa.
23. L. J. Schreiner, “Review of Fricke gel dosimeters”, *Journal of Physics: Conference Series*, 2004.
24. H. Fricke and E. Hart „Chemical Dosimetry“, *Radiation Dosimetry* vol.2, Academic Press, New York, 1955.
25. C. Duzenli, R. Sloboda, D Robinson „A spin-spin relaxation rate investigation of the gelatin ferrous sulphate NMR dosimeter“, *Physics in Medicine & Biology*, 1994.
26. W. I. D. Rae, C. A. Willemse, M. G. Lotter, S. Engelbrecht, J. C Swarts,1996“ Chelator effect on ion diffusion in ferrous-sulphate doped gelatin gel dosimeters as analyzed by MRI“, *Medical Physics*, 1996.
27. M. Lepage, K. Jordan, „3D dosimetry fundamentals: gels and plastics“, *Journal of Physics: Conference Series*, 2010.
28. Y. De Deene, C. Hurley, A. Venning, K. Vergote, M. Mather, B. J. Healy, C. Baldock, „A basic study of some normoxic polymer gel dosimeters“, *Physics in Medicine & Biology*, 2002 September.
29. P. M. Fong, D. C. Keil, M. D. Does, J. C. Gore, „Polymer gels for magnetic resonance imaging of radiation dose distributions at normal room atmosphere“, *Physics in Medicine & Biology*, 2001 November.
30. M. M. T. Khan, A. E. Martell, „Metal ion and metal chelate catalyzed oxidation of ascorbic acid by molecular oxygen. I. Cupric and ferric ion catalyzed oxidation“, *Journal of the American Chemical Society*, 1967 August.
31. V. Spěváček, K. Pilařová, J. Končeková , O. Konček, „The influence of antioxidant THPC on the properties of polymer gel dosimeter”, *Physics in Medicine & Biology*, 2014 August.
32. Y. Watanabe, L. Warmington, N. Gopishankar, „Three-dimensional radiation dosimetry using polymer gel and solid radiochromic polymer: From basics to clinical applications“, *World Journal of Radiology*, 2017 March.
33. K. B. McAuley „Fundamentals of Polymer Gel Dosimeters“, *Journal of Physics: Conference Series*, 2006.

34. M. Lepage, P. M. Jayasakera, S A° J Bäck, C. Baldock, „Dose resolution optimization of polymer gel dosimeters using different monomers“, *Physics in Medicine & Biology*, 2001 September.
35. M. J. Maryanski, J.C. Gore, R. P. Kennan, R Schulz , „NMR relaxation enhancement in gels polymerized and cross-linked by ionizing radiation: a new approach to 3D dosimetry by MRI“, *Magnetic Resonance Imaging*, 1993
36. K. B. McAuley „The chemistry and physics of polyacrylamide gel dosimeters: why they do and don't work“, *Journal of Physics: Conference Series*, 2004.
37. Y. De. Deene, K. Vergote, C. Claeys, C. De Wagter, „The fundamental radiation properties of normoxic polymer gel dosimeters: a comparison between a methacrylic acid based gel and acrylamide based gels“, *Physics in Medicine & Biology* , 2006 January.
38. Y De Deene, „Essential characteristics of polymer gel dosimeters“, „*Journal of Physics: Conference Series"*, 2004.
39. M. Aljamal, A. Zakaria, S. Shamsuddin, „Radiological properties of MAGIC normoxic polymer gel dosimetry“, *Journal of Physics: Conference Series*, 2013.
40. G.S. Ibbott, „Clinical Applications of Gel Dosimeters“, *Journal of Physics: Conference Series*, 2006.
41. M. Oldham, I. Baustert, C. Lord, T. A. Smith, M. McJury, A. P. Warrington, M. O. Leach, S. Webb „An investigation into the dosimetry of a nine-field tomotherapy irradiation using BANG-gel“, *Physics in Medicine and Biology*, 1988.
42. P. A. Love, P. M. Evans, M. O. Leach, S. Webb „Polymer gel measurement of dose homogeneity in the breast: comparing MLC intensity modulation with standard wedged delivery“. „*Medical Physics*, 2003 April.
43. J. V. Trapp, M. Partridge, V. M. Hansen, P. Childs, J. Bedford, A. P. Warrington, M. O. Leach, S. Webb, „The use of gel dosimetry for verification of electron and photon treatment plans in carcinoma of the scalp“, *Physics in Medicine and Biology*, 2004 May.
44. M. Hassan, A. U. Rehman, M. M. Waheed, M. N. Anjum, „Dose of radiation enhancement, using silver nanoparticles in a human tissue equivalent gel dosimeter“, *The Journal of the Pakistan Medical Association*, 2016 January.
45. S. Rosa, C. Connolly, G. Schettino, K. T. Butterworth, K. M. Prise, „Biological mechanisms of gold nanoparticle radiosensitization", *Cancer Nanotechnology Basic, Translational and Clinical Research*, 2017 January.
46. https://oncohemakey.com/principles-of-radiologic-physics-and-dosimetry/

47. H. Khosravi, B. Hashemi, F Rahmani, „Gel dosimetry: The effect of gold nanoparticles on the dose enhancement in the external radiation therapy“, *Nanomedicine Research Journal*, 2016 July.
48. E. J. Jabaseelan Samuel, K Srinivasan, V. Poopathi, „Radiation dose enhancement of gold nanoparticle on different polymer gel dosimeters“, *Journal of Physics: Conference Series*, 2017.
49. T. Marques, M. Schwarcke, C. Garrido, V. Zucolotto, O. Baffa, P. Nicolucci, „Gel Dosimetry Analysis of Gold Nanoparticle Application in Kilovoltage Radiation Therapy“, *Journal of Physics: Conference Series*, 2010
50. M. Y. Chang, A. L. Shiau, Y. H. Chen, C. J. Chang, H. Chen, C. L. Wu1, „Increased apoptotic potential and dose-enhancing effect of gold nanoparticles in combination with single-dose clinical electron beams on tumor-bearing mice“, *Cancer Science*, 2008 July.
51. A. M. Ealias, M. P. Saravanakumar „A review on the classification, characterisation, synthesis of nanoparticles and their application“ *IOP conference series: Materials Science and Engineering* 2017
52. *S.* Iravani, H. Korbekandi, S.V. Mirmohammadi, B. Zolfaghari, „Synthesis of silver nanoparticles: chemical, physical and biological methods“, *Research in Pharmaceutical Sciences*, 2014 November.
53. M. Darroudi, M. B. Ahmad, A. K. Zak, R. Zamiri, M. Hakimi, „Fabrication and Characterization of Gelatin Stabilized Silver Nanoparticles under UV-Light“, *International Journal of Molecular Sciences*, 2011 September.
54. A. Abedini, A. R. Daud, M. A. A. Hamid, N. K. Othman, E. Saion „A review on radiation-induced nucleation and growth of colloidal metallic nanoparticles“, *Nanoscale Researc Letters*, 2013.
55. J. Luci, H. M. Whitney, J. C. Gore, „Optimization of MAGIC gel formulation for three-dimensional radiation therapy dosimetry“, *Physics in Medicine & Biology*, 2007 May.
56. N. R. Kakade, S. D. Sharma „Dose enhancement in gold nanoparticle‑ aided radiotherapy for the therapeutic photon beams using Monte Carlo technique“, *Journal of Cancer Research and Therepeutics*, 2015 April.
57. http://www.gafchromic.com/documents/RTQA2_Literature.pdf
58. http://www.gotopeo.com/images/stories/pdf/rt/isp_ebt2productspec_09_peo.pdf
59. http://www.ptwusa.com/typo3conf/ext/naw_securedl/secure.php?u
60. USB4000 Fiber Optic Spectrometer Installation and Operation Manual Document Number 211-00000-000-02-0908.
61. H. Cen, R. Lu „Optimization of the hyperspectral imaging-based spatially-resolved system for measuring the optical properties of biological materials“, *Optics Express*, 2010.

APPENDIX 1

Table.1. Treadline eqations and R^2 values from graphs, where presented results using film.

Gel name	Trendline equation and R^2 (GafChromic RTQA^{2}film results)	Trendline equation and R^2 (GafChromic EBT2 film results)
MAGIC(S) Control	y=0.0433x+0.4489; R^2=0.9478 y=0.0349x+0.4313; R^2=0.9506	y=0.0604x+0.0406; R^2=0.961 y=0.0494x+0.373; R^2=0.979
Gelatin($AgNO_3$) Control	y=0.0373x+0.467; R^2=0,9489 y=0.0349x+0.4313; R^2=0.9506	y=0.0529x+0.4294; R^2=0.9746 y=0.0494x+0.373; R^2=0.979
Gelatin(NPs1mM) Control	y=0.0376x+0.4612; R^2=0.9668 y=0.0349x+0.4313; R^2=0.9506	y=0.0506x+0.4333; R^2=0.9693 y=0.0494x+0.373; R^2=0.979
MAGIC(3%) Control	y=0.026x+0.5727; R^2=0.826 y=0.0263x+0.5662; R^2=0.8288	-
MAGIC(6%) Control	y=0.032x+0.5165; R^2=0.8281 y=0.0319x+0.5151; R^2=0.8193	
MAGIC(9%) Control	y=0.0322x+0.5178; R^2=0.8365 y=0.032x+0.5147; R^2=0.8472	
MAGIC(NPs20mM) Control	y=0.0576x+0.4184; R^2=0.9748 y=0.0427x+0.3612; R^2=0.9813	
MAGIC(NPs10mM) Control	y=0.0573x+0.4157; R^2=0.9748 y=0.0427x+0.3612; R^2=0.9813	
MAGIC(NPs2mM) Control	y=0.0248x+0.4974; R^2=0.9377 y=0.0255x+0.4972; R^2=0.9458	
MAGIC(NPs1mM) Control	y=0.0244x+0.4956; R^2=0.9352 y=0.0251x+0,4966; R^2=0.9393	
MAGIC(NPs5mM) Control	y=0.0244x+0.4987; R^2=0.9443 y=0.0243x+0.4934 R^2=0.9362	

Table.2. Treadline eqations and R^2 values from graphs, where presented absorption coefficient.

Gel name	Trendline equation and R^2 (unirradiated)	Trendline equation and R^2 (irradiated)
MAGIC(6%)	y=-0.0108x2+0.1248x+24.645 R^2=0.6804	y=-0.0186x^2+0.0829x+24.5754 R^2=0.9232
MAGIC(NPs2mM)	y=-0.0216x^2+0.2146x+26,068 R^2=0.9339	y=-0.0313x^2+0,299x+25.986 R^2=0.9947